Spatial Proteomics Reveals Novel TREM2 Interactors in ER-Mitochondria Interface in Microglia

Chulhwan Kwak,[1,2,8] Gina M. Finan,[4,8] Yu Rim Park,[5,6] Ji Young Mun,[5,6*], Hyun-Woo Rhee,[1,3*] Tae-Wan Kim[4,9*]

[1]Department of Chemistry, Seoul National University, Seoul 08826, Korea
[2]The Research Institute of Basic Science, Seoul National University, Seoul 08826, Korea
[3]School of Biological Sciences, Seoul National University, Seoul 08826, Korea
[4]Department of Pathology and Cell Biology, Taub Institute for Research on Alzheimer's Disease and the Aging Brain, Columbia University Irving Medical Center, New York, NY 10032, USA
[5]Division of Biomedical science, School of Medicine, Kyungpook National University, Daegu, Republic of Korea
[6]Neural Circuit Research Group, Korea Brain Research Institute, 41062 Daegu, Korea
[7]Present address: Department of Neurosurgery, Stanford University School of Medicine, Stanford, CA, USA
[8]These authors contributed equally.
[9]Lead contact
*Correspondence: jymun@kbri.re.kr (J.Y.M), rheehw@snu.ac.kr (H.-W.R.), twk16@cumc.columbia.edu (T.-W.K.)

SUMMARY

Triggering receptor expressed on myeloid cells 2 (TREM2) plays a central role in microglial biology and the pathogenesis of Alzheimer's disease (AD). Besides DNAX-activating protein 12 (DAP12), a communal adaptor for TREM2 and many other receptors, other cellular interactors of TREM2 remain largely elusive. We employed a 'proximity labeling' approach using a biotin ligase, TurboID, and discovered novel TREM2-proximal proteins, many of which localized to the Mitochondria-ER contact sites (MERCs). TREM2 deficiency alters the thickness (inter-organelle distance) of MERCs, a structural parameter of metabolic state, in microglia derived from human induced pluripotent stem cells. Our TurboID-based TREM2 interactome study suggest novel roles for TREM2 in the regulation of MERCs, raising the possibility that dysregulation of MERC-related TREM2 functions contribute to AD pathobiology.

INTRODUCTION

Alzheimer's disease (AD) is the leading cause of dementia in the elderly. In addition to plaques, tangles, and widespread neuronal death, there are profound inflammatory changes in the AD brain, which are increasingly presenting new therapeutic targets (Fu et al., 2019; Wyss-Coray and Mucke, 2002). Microglia act as the brain's immune cells, representing roughly 10% of the cells in the brain, and are becoming the subject of intense investigation in the field of neurodegenerative disease research (Leng and Edison, 2021; Hansen et al., 2018; Sarlus et al., 2017). In AD, microglia are linked closely to all pathological cascades including amyloid, tau and neuroinflammatory changes (McQuade and Blurton-Jones, 2019). Recent genome-wide association studies (GWAS) revealed that a number of AD risk genes are highly (and often exclusively) expressed in microglia, including the gene encoding triggering receptor expressed on myeloid cells-2 (TREM2) (Colonna, 2023; Villegas-Llerena et al., 2016; Griciuc and Tanzi 2021; Jorfi et al., 2023). Notably, a rare R47H hypomorphic mutation in the TREM2 increases the risk of AD several fold (R. Guerreiro et al., 2013; Jonsson et al., 2013). Gene network studies reveal that TREM2 and its adapter protein, DNAX-activation protein 12 (DAP12; also known as TYROBP) strongly associate with AD (Zhang et al., 2013; 2016; Matarin et al., 2015). Homozygous variants in TREM2 or its binding partner DAP12 are also shown to cause Nasu-Hakola disease (NHD) with early-onset dementia (Paloneva et al., 2002; Klunemann et al., 2005). Despite the strong clinical phenotype of human NHD, TREM2-deficient and DAP12-deficient mice do not exert strong NHD-like phenotypes (Zhou et al., 2023).

TREM2 is a transmembrane immune signaling receptor, which serves as a receptor for β-amyloid (Zhao et al., 2018; Lessard et al., 2018; Zhong et al., 2018) and various lipoproteins including high density lipoprotein containing apolipoprotein E (Song et al., 2017; Atagi et al., 2015; Bailey et al., 2015). TREM2 promotes the survival and proliferation of microglia and mediates the clearance of apoptotic neurons via phagocytosis without inducing apparent neuroinflammation (Takahashi et al., 2005). TREM2 is essential for retaining a fully mature disease-associated microglia (DAM) profile and for supporting the microglial response to Aβ-plaque-induced pathology (Keren-Shaul et al., 2017; Krasemann et al., 2017). TREM2-dependent response requires the induction of the phosphorylation of tyrosine residues within the

ITAM motifs of DAP12, by Src-family kinases and downstream signaling cascades including AKT and mTOR (Kober et al., 2017; Jay et al., 2017).

Despite extensive investigation, we currently do not have a complete mechanistic understanding of microglial TREM2 signaling, due in part to the lack of a comprehensive knowledge of TREM2-bearing molecular complex(es) in microglial cells. Most of the focus has been on the interaction of TREM2 with DAP12, which serves as a communal platform for downstream signaling. In addition to TREM2, DAP12 has been shown to interact with numerous receptors (Lanier, 2009). Given the complexity and high disease relevance of TREM2-associated biological processes, it is conceivable that additional molecular components may interact with TREM2 and contribute substantially to the regulation of relevant microglial functions. To this end, we set out to identify novel components of TREM2-harboring protein complex(es), not yet implicated in TREM2 signaling, using an unbiased proteomics approach.

Our experimental approach used the TurboID-based "proximity labeling (PL)" technique to investigate the protein-protein interactions in living microglial cells (Lam et al., 2015; Han and Ting, 2018; Lee et al., 2019; Qin et al., 2021; Choi and Rhee, 2022). TurboID, an engineered biotin ligase, uses ATP to convert biotin into biotin-AMP, a reactive intermediate that covalently labels biotin to the proximal proteins (Doerr, 2018; Brandon et al., 2018). Using the human microglial cells stably expressing TurboID-fused to the cytoplasmic region of TREM2, we performed proximity labeling experiments followed by mass spectrometry analysis, and successfully identified and validated 47 putative TREM2 interacting proteins. Interestingly, among these proteins, 21 proteins are found to localize to the subcellular compartment known as the mitochondria-ER contacts (MERCs) (Vance 1990; 2014; Lee et al., 2018). Biochemically isolated MERCs are also referred to as mitochondrial associated membranes (MAMs; Vance 2014). MERCs have been implicated in many functional roles associated with TREM2, including lipid transport, mitochondrial energy metabolism, Ca^{2+} handling and immune sensing (Rieusset, 2018; Tubbs and Rieusset, 2017), and have also been suggested to be a pathological hub for several neurodegenerative diseases, including AD (Area-Gomez et al., 2018; Bose and Beal, 2016; Paillusson et al., 2016; Johri and Chandra, 2021; Area-Gomez and Schon, 2017). Given the physical and/or functional association of TREM2 to MERC-related cellular activities, we investigated the effects of TREM2 deficiency on the cell biological changes of MERCs in the human induced pluripotent stem cells (iPSC)-derived microglia (iMGL) (Abud et al., 2017; McQuade et al., 2018). TREM2 deficiency leads to the ultrastructural alteration of MERCs, further supporting a functional association of TREM2 to MERCs. Our finding also raises the possibility that TREM2-mediated microglial functions relevant to AD may be attributed to the aberrant regulation of MERCs in microglia.

RESULTS

Proximity labeling activity of TREM2-TurboID in human microglial cell line

For enzyme-based proximity labeling (PL), we selected TurboID, one of the engineered biotin ligases that is suitable for protein-protein interaction mapping due to the high catalytic activity as

compared to other PL enzymes (Branon 2018). We generated mammalian expression plasmids encoding human TREM2 fused to a C-terminal V5 tag and TurboID (TREM2-V5-TurboID) (Figure 1A). TREM2-V5-TurboID was transfected into the human microglial cell line, IM-HM (Mazzeo et al., 2022). Western bloting with antibodies against V5-tag or TREM2 revealed that TREM2-V5-TurboID is expressed with the predicted size (Figure 1B). Confocal fluorescent microscopy showed that TREM2-V5-TurboID localizes mainly to intracellular compartments as previously reported (Figures 1C; Kleinberger 2014; Park 2015; Yin 2016; Zhao 2017). We next performed confocal microscopy analysis to detect subcellular distribution of TREM2-V5-TurboID-mediated biotinylation using streptavidin-647 (Figure 1C). TREM2-V5-TurboID immunoreactivity and biotin-labeled signals appear to co-localize strongly, suggesting that the biotin labeling occurs at subcellular compartments in close proximity to TREM2-V5-TurboID. TurboID conjugated to nuclear export signal and V5 tag (V5-TurboID-NES) was used as a control, and the biotin signals from V5-TurboID-NES vs TREM2-V5-TurboID occurred in spatially distinct subcellular sites (data not shown). We next biochemically validated PL activity of TREM2-V5-TurboID in IM-HM cells. Upon incubation with exogenous biotin, a wide range of biotinylated proteins were detected in TREM2-V5-TurboID-expressing cells (Figure 1D). The biotin-labeled proteins were then analyzed by Western blotting using streptavidin-HRP. Distinct patterns of biotinylated proteins were observed in the samples from the V5-TurboID-NES-expressing IM-HM cells.

Proximal proteomics of TREM2 in living microglial cells

We performed PL experiments similar to the processes that we previously described (Figure 1A; Lee et al., 2019; Kwak et al., 2020). We established stable IM-HM transfectants expressing TREM2-V5-TurboID and performed biotin labeling. The samples were subjected to streptavidin pull-down to enrich biotin-conjugated proteins. We then performed ‘Spot-TurboID’, which involves on-bead trypsin digestion, allowing direct mass spectrometry analysis of the peptide harboring biotin-conjugated lysine (K+226) (Lee et al., 2019). This approach removes the bulk of unlabeled peptides, therefore drastically improving detection sensitivity and reducing false positive results. After verifying the biotin labeling, biotin-labeled peptides were analyzed by mass spectrometry as previously described (Lee et al., 2019; Kwak et al., 2020). By statistically assessing the relative enrichment of the biotinylated peptides from TREM2-V5-TurboID relative to the control (V5-TurboID-NES), we identified 47 proteins as components of a TREM2 interactome (Figure 2A).

Analysis and validation of TREM2 interactome

Quantification of biotinylated peptides derived from the TREM2 proximal proteins was performed as previously described (Lee et al., 2019). Our TREM2 interactome analysis revealed a total of 47 proteins (Figure 2A). To our surprise, among the 47 identified proteins, we found that 21 TREM2-proximal proteins are known components of MERCs (Figure 2B). These MERC components were identified in a previous study via ER-OMM contact-dependent localization studies (Kwak et al., 2020). Quantitative proteomics allowed us to determine the MS signal intensity of MERC components vs. non-MERC components (Figures S2). Our assessment of the TREM2-TurboID interactome reveals novel TREM2 interactors in the MERCs of a human

155 microglial cell line. We summarized the TREM2 interactome and their corresponding subcellular
156 sites (Figure 2C).
157
158 To validate the physical proximity of TREM2-V5-TurboID and identified proteins, we performed
159 a direct biotinylation assay using the expression plasmid encoding each “hit” protein (Figure
160 S1A). An expression construct encoding TREM2-V5-TurboID was co-transfected with each
161 expression “hit” construct in 293 cells and subjected to in situ biotinylation assay for validation.
162 This assay successfully validated the interaction between TREM2-V5-TurboID and the well-
163 known TREM2 interactor, DAP12, as well newly discovered interactors such as CISD2 and
164 CKAP4 (Figure S1B). PL-mediated biotin incorporation is shown to be quantitative (Han and
165 Ting, 2018; Choi and Rhee, 2022). DAP12 exhibited the highest levels of biotin incorporation as
166 compared to other identified components of TREM2 interactome (Figure S1B). Our 47
167 confirmed TREM proximal proteins were found to be positive.
168
169 **TREM2 localization to the MERCs**
170 We next investigated the subcellular localizations of TREM2-proximal proteins. To precisely
171 map the MERCs, we used ‘Contact-ID’, in which two inactive fragments of BioID (a PL enzyme),
172 are reconstituted via protein-protein interaction across two distal membranes and become
173 catalytically active (Figure 3A; Kwak et al., 2020). The Contact-ID system consists of the N-G78
174 (B1) fragment of BioID conjugated to the cytosol-facing N terminus of SEC61B (B1-SEC61B) at
175 the ER membrane and the G79-C (B2) fragments of BioID conjugated to the C terminus of
176 TOM20 (TOM20-B2) at the OMM. This approach allows for precise mapping of the MERC
177 contact sites without overlapping distribution of virtually any MERC components with either the
178 ER or OMM. We transfected TREM2-V5 without TurboID and examine the subcellular
179 distribution of TREM2 vs. Contact-ID-dependent signals (Figure 3B). Confocal microscopy
180 analysis showed that the subcellular localization pattern of TREM2 overlaps substantially to that
181 of the Contact-ID signal. Biochemical data showed that TREM2 is indeed proximal to the MERC
182 components (Figure 3C). These data suggest that TREM2 localizes to the MERCs and
183 biotinylation of TREM2 is mediated by the PL activity of TREM2-TurboID within the MERCs.
184
185 **Ultrastructural Analysis of MERCs in TREM2-deficient iMGL**
186 Prevalent localization of the TREM2 interactome in the MERCs suggests that TREM2 may be
187 required for the proper structural and/or functional regulation of MERCs in human microglia.
188 Recently, human induced pluripotent stem cell (iPSC)-derived microglial models (iMGL) for AD
189 became available (Abud et al., 2017; McQuade et al., 2018). We therefore investigated the cell
190 biological impact of TREM2 deficiency in human iMGL -a more physiological model system as
191 compared to a microglial cell line. We performed electron microscopy analysis to test if TREM2
192 deficiency affects the ultrastructure of MERCs in iMGL (Figure 4). As shown in the previous
193 studies (Nugent et al., 2020), there is a marked increase of lipid droplets (LDs) in TREM2-
194 deficient iMGL as compared to wild-type iMGL (Figure S3). We next performed morphological
195 characterization of MERCs in wild-type vs. TREM2 deficient iMGL (Figure 4A). We found that
196 overall MERC thickness is greatly increased in TREM2 knockout iMGL as compared to wild-
197 type (Figure 4B, 4C). The established key structural parameter of MERCs includes the width of
198 the gap (10-30 nm distance) between cytosolic sites of ER membrane and OMM (MERC

thickness; Csordás et al., 2006; Giacomello and Pellegrini, 2016). MERC thickness is a regulated parameter strongly associated with metabolic state of the cells. Cell function and survival relies on the maintenance of a proper spacing between the ER and mitochondria (Csordás et al., 2006; Giacomello and Pellegrini, 2016). To ensure that the observed increases of the MERC thickness in the TREM2-deficient iMGL is specific to cell biological alterations due to TREM2, we next tested whether re-introduction of TREM2 into the TREM2-deficient iMGL could restore the observed MERC alterations associated with TREM2 deficiency (Figure 5). Lentiviral delivery of TREM2 in the TREM2 deficient iMGL leads to a decrease in the MERC thickness as compared to iMGLs infected with control lentiviral particles (Figure 5). In addition, the MERC thickness increased occurrence of LDs, a prominent phenotype of TREM2-deficient iMGL, was also rescued by the introduction of wild-type human TREM2 (Figure S4). These data suggest that the increased MERC thickness in the TREM2-deficient cells is a TREM2- specific cell biological change.

Effects of R47H TREM2 on the MERC thickness

We next analyzed the MERC thickness of the iMGL derived from human iPSC carrying the R47H TREM2 variant (Figure 6A). We determined the distance of ER-to-mitochondria of iMGL carrying TREM2 R47H mutant, as compared to isogenic wild-type control. The MERC thickness was significantly elevated in the TREM2 R47H iMGL relative to control (Figure 6B). The MERC thickness phenotype was less profound than that observed in the TREM2 full knockout iMGL, probable due to the partial loss-of-function characteristics of TREM2 R47H (Cheng-Hathaway et al., 2018; Sudom et al., 2018). The occurrence of LDs was also increased in the iMGLs carrying R47H TREM2 as compared to isogenic wild-type (Figure S4).

DISCUSSION

Protein interaction networks underlie the biological processes and pathological progression of human diseases (Rees et al., 2015; Bludau and Aebersold, 2020). Given the critical role for TREM2 in microglial biology as well as the pathophysiology of AD, a comprehensive understanding of the protein-protein interaction networks of TREM2 should provide new insights on TREM2 functions in microglia. We utilized an TurboID-catalyzed PL approach combined with mass spectrometry to determine the TREM interactome in live microglial cells. The PL approach overcomes some inherent limitations of the traditional methods associated with co-immunoprecipitation combined with mass spectrometry and yeast two-hybrid assays, which often involve a post-lysis manipulation of the starting material (e.g. detergent extraction, subcellular fractionation). PL can detect native protein-protein interactions in live cells, and is thereby highly suitable for mapping target protein interactome with a greater specificity. Among a number of PL enzymes, turboID was chosen because of its catalytic efficiency, simplicity and the use non-toxic biotin substrate (Branon et al., 2019). Here we identified novel proteins proximal to TREM2-TurboID, including those localized predominantly to MERCs, unveiling the connection between TREM2 and MERCs.

MERC is a dynamic and plastic structure that can undergo remodeling in response to metabolic change and stress (Rowland 2012; Csordás et al., 2006). The thickness of MERC, the width of

243 the cleft that separates the ER and OMM, is considered a regulated structural parameter that
244 changes depending on the metabolic state of the cells (Giacomello and Pellegrini, 2016).
245 Changes in the width of the cleft in MERC influence the lipid transfer process across two
246 membranes (Giacomello and Pellegrini, 2016). We have demonstrated that deficiency or
247 hypomorphic R47H mutation of TREM2 lead to increased thickness of MERCs in iMGs (Figures
248 4 and 6). In addition to our novel observation of the MERC alterations, our results show the
249 increased occurrence of LDs in TREM2 deficient iMGL (Figure S3). This is consistent with the
250 previous report demonstrating the increased accumulation of cholesterol ester (e.g. CE20:4 and
251 CE22:6), the major cholesterol metabolites stored in LDs, in both mouse brain and cultured
252 human myeloid cells (Nugent et al., 2020). Since MERC has been shown to play an important
253 role in the biogenesis of LD (Liu et al., 2015; Freyre et al., 2019; Choudhary et al., 2021; Guyard
254 et al., 2022), it is conceivable that altered MERC in the TREM2 deficient iMGL may be attributed
255 to the aberrant accumulation of LDs in iMGL. When cell conditions promote active expansion of
256 LDs, the synthesis and trafficking of new phospholipids are regulated in the area between
257 mitochondria and ER (Olzmann et al., 2019). According to a report by Area-Gomez et al., the
258 ACAT protein relating LD generation was more abundant in the mitochondria-associated ER
259 membranes (MAMs) fraction and had approximately 3 times higher enzymatic activity compared
260 to the ER and mitochondrial fractions (Area-Gomez et al., 2012). Collectively, virtually all known
261 TREM2 functions including metabolic regulation of lipids and Ca^{2+}, as well as inflammatory
262 activation, are linked intimately to those of MERC, substantiating the idea that TREM2 is an
263 important factor for proper MERC functions.
264
265 Aberrant MERCs have been reported in cellular models of AD. Gene deletion and FAD
266 mutations of familial AD-associated presenilin genes (PSEN1 and PSEN2) greatly increases the
267 MERC thickness (50-200 nm) in fibroblasts (Area-Gomez et al., 2012). Presenilin 2 has been
268 shown to regulate Ca^{2+} crosstalk across the MERCs (Zampese et al., 2011). PS1 has also been
269 shown to interact with TREM2 (Zhao et al., 2017). In addition to AD, MERCs have been
270 implicated in other neurodegenerative diseases, such as Parkinson's disease (PD) (Area-
271 Gomez et al., 2018; Bose and Beal, 2016; Paillusson et al., 2016; Johri and Chandra, 2021;
272 Area-Gomez and Schon, 2017). Occurrence of the microglial TREM2 interactome in the MERCs
273 is particularly relevant to a known MERC functions involving immune activation. MERC is shown
274 to serve as a signaling hub for NLRP3 inflammasome activation (Horng et al., 2014; Zhou et al.,
275 2020). TREM2 is a direct regulator of the NLRP3 inflammasome and the AD-linked R47H
276 TREM2 variant is not capable of activating the inflammasome (Cosker et al., 2021; Li et al.,
277 2021; Jiang et al., 2022; Wang et al., 2022). These observations further substantiate the idea of
278 the central role for TREM2 in regulating MERC functions.
279
280 In our previous study, we developed Contact-ID, a split-pair BioID system used to identify the
281 protein components of MERCs (Kwak et al., 2020). Since all known MERC markers show
282 overlapping subcellular distribution in either the ER or OMM, the Contact-ID approach allows
283 precise mapping of ER-OMM contact-dependent localization (Figure 3), indicting co-localization
284 of TREM2 with identified MERC components in the TREM2 interactome. In addition to the
285 components of MERC, our PL interactome study revealed newly discovery TREM2-interacting
286 proteins with distinct subcellular localizations (Figure 2E), suggesting potential mediators or

modulators of cellular functions of TREM2 in microglial cells. For instance, anoctamin 6 encoded by ANO6 is an essential component for Ca2+-dependent exposure of phosphatidylserine (PS) on the cell surface (Yang et al., 2012; Kunzelmann et al., 2014). PS exposure is considered to be one of the “eat-me” signals for the engulfment by immune cells (Lemke et al., 2019; Scott-Hewitt et al., 2020) and ANO6 has been shown to increase microglial phagocytosis of neurons (Batti et al., 2016; Zhang et al., 2020). Interestingly, ANO6 deficiency reduces activation of the microglial NLRP3 inflammasome in the brain of AD mouse model (Cui et al., 2023), suggesting the functional link of ANO6 with TREM2 in the regulation of NLRP3 inflammasome (Li et al., 2021; Jiang et al., 2022). CDK5 regulatory subunit Associated protein 1-Like 1 (CDKAL1) has been implicated in the pathogenesis of type2 diabetes (Ghosh et al., 2022) and a family-based GWAS meta-analysis revealed genetic association of two SNPs in the *CDKAL1* gene (Herold et al., 2016). ITPRIP gene (The gene encoding inositol 1,4,5-trisphosphate receptor interacting protein) has also been suggested as an AD risk gene (Simino et al., 2017). AUP1 and REEP5 are known to play a key role in LD biogenesis (Robichaud et al., 2021; Chen et al., 2022), consistent with the functional role for TREM2 in the LD biogenesis. Collectively, our current study provides new insights on TREM2 functions and serves as a foundation for further research aimed at deciphering new molecular players in microglial TREM2 functions.

Limitations of the study

-We haven’t done functional analysis of other non-MERC interactors.
-We did not cover the aspect of interactome mediated by TREM2 ectodomain.
-Our study requires further validation in vivo.

ACKNOWLEDGMENTS

Use this section to acknowledge contributions from non-authors and list funding sources. If this work was enabled due to contributions of a core facility or shared resource at your institution, we encourage you to acknowledge those contributions as well. As this section contains important information and many funding bodies require inclusion of grant numbers here, please check it carefully.

AUTHOR CONTRIBUTIONS

This section is required for all papers. Please use it to concisely describe each author’s contributions, using initials to indicate each author’s identity. We encourage you to use the CRediT taxonomy, but you can also use a traditional format (e.g., "A.B. and C.D. conducted the experiments; E.F. designed the experiments and wrote the paper.").

DECLARATION OF INTERESTS

This section is required for all papers. Please use it to disclose any competing interests, in accordance with Cell Press's declaration of interests policy. If there are no interests to declare, please note that with the following wording: "The authors declare no competing interests." The text in this section should match the text provided in the declaration of interests form. https://www.cell.com/pb/assets/raw/shared/forms/di_form.pdf

STAR+METHODS

Culture of iMGL

The wild type iMGL, TREM2 deficient iMGL, and iMGL derived from human iPSC carrying R47H TREM2 variant (Fujifilm Cellular dynamics iCell microglia, AHN, TREM2 R47H, #11969) were cultured in iCell microglia media kit (Fujifilm cellular dynamics, USA, #R1204) as recommended by a manufacturer. Cells were maintained on 0.07 % Poly ethyleneimine solution coated plate in suspension. For re-introduction of TREM2 into the TREM2-deficient iMGL, TREM2-deficient iMGL was infected with two different lentiviral particles (Control lentiviral particles (CH404_empty_GFP reporter_pDual) and TREM2 delivery lentiviral particles (CH400_ss-V5-TREM2-twin strep tag_GFP reporter_pDual)).

Transmission electron microscopy (TEM) analysis

Cells were pre-fixed with 2% paraformaldehyde/2.5% glutaraldehyde and post-fixed in 2% Osmium tetroxide (OsO4; EMS, USA). After block staining with 1.5% potassium ferrocyanide (sigma, USA), 1% thiocarbohydrazide (TCH; TCI, Japan), 2% OsO4, and 2% uranyl acetate (EMS, USA), dehydration with a graded ethanol series (20%, 50%, 70%, 90%, and 100%) and infiltration with an epoxy resin (30, 50, 70, and 100%) were done. Then, samples were embedded with an EMBed-812 embedding kit (EMS, USA) following the manufacturer's instructions. Cells were sectioned at 60 nm using an ultramicrotome (UC7; Leica Microsystems, Germany) and sections were mounted on copper slot grids with a formva film. The sections were imaged by the Tecnai G2 microscope with a US1000X-P camera 200 (Thermo Fisher Scientific, USA) at an accelerating voltage of 120 kV.

Analysis of MERCs in iMGL

Ultrastructural analysis of MERCs in iMGL was performed as previously described (Giacomello et al., 2016; Raturi et al., 2016; Bartok et al., 2019) The thickness of MERCs with less than 30 nm between the mitochondria and ER was measured in 10 regions of MERCs. MERCs thickness and length in each group were determined in nanometers and averaged. Data were analyzed using a Image J software. Statistical analysis was performed using GraphPad Prism 8 software (GraphPad Software Inc., LaJolla, CA). The statistical significance was $p < 0.001$.

Analysis of lipid droplets in iMGL

To identify the number of lipid droplets (LDs), cells were stained with Lipi-red (Dojindo, Japan; 1 umol/L) and Hoechst solution (Sigma, USA; 1 umol/L). Live cells were imaged under a confocal light microscopy (Ti-RCP, Nikon, Japan). The ultrastructure of LDs was observed under a TEM and the number of LDs was measured by Image J software.

FIGURE LEGENDS

Figure 1. TurboID-based proximity labeling of TREM2 in microglial cells.

(A) Schematic workflow of proximity labeling, spot-ID, mass spectrometry and in situ TREM2 interactome mapping.

(B) Western blot analysis of the samples from the IM-HM microglial cells transfected with the expression constructs: human wild-type or R47H version of TREM2 with C-terminal V5 tag and TruboID and mCherry-V5.

(C) Confocal microscopy analysis of IM-HM cells transfected with TREM2-V5-TurboID using anti-V5 antibodies or with Streptavidin-647 for the detection of biotin-labeled protein.

(D) Streptavidin-HRP blot detection of biotin-labeled proteins in the samples from the IM-HM cells transfected with TREM2-V5-TurboID construct.

Figure 2. Clustering of TREM2 interactome.

(A) Volcano plots showing statistically significant enrichment of biotinylated proteins (group-TREM2-TurboID) over the cytosolic biotinylated proteins by NES-TurboID (TREM2 interactome). Among the TREM2 interactome, MERC components are also indicated. Enrichment of the Spot-TurboID detected biotinylated proteins by TREM2-V5-TurboID. x-axis: Log2 value of fold change (FC) of mass signal intensities. Cut off value is 1.2; y-axis: -Log10 value of p-value, cut off value is 1.2.
(B) Segregation of TREM2 interactome vs. previously known MERC components shown by Contact-ID (Kwak et al., 2020).
(C) Subcellular distribution of TREM2 interactome proteins across the MERC (MAM), ER, mitochondria, secretory vesicles, Golgi and cell surface.

Figure 3. TREM2 localization in the MERCs.
(A) Schematic diagram of Contact-ID for MERC mapping using split BioID.
(B) Confocal microscopy imaging of MERC biotinylation by Contact-ID in HEK293T cells. TREM2 was visualized by anti-V5 antibody. Biotinylated proteins were visualized by AF647-conjugated streptavidin.
(C) Streptavidin-horseradish peroxidase (SA-HRP) Western blot of biotinylated proteins.

Figure 4. Analysis of MERCs in wild type iMGL and TREM2 deficient iMGL.
(A) Transmission Electron microscopy (TEM) images of wild-type and TREM2 deficient iMGL cells. Red boxes are enlarged images of dotted area. Each ultrastructure of intracellular organelles including mitochondria and ER is intact without abnormality. scale bar: 1 um.
(B) The thickness and length of MERC were analyzed in each group. Red arrows represent MERC. The thickness of MERCs with less than 30 nm between the mitochondria and ER was measured in 10 regions of MERCs.
(C) The averaged thickness was significantly increased in TREM2 deficient iMGL, and the thickness (nm) was each 14.66 ± 0.5824 and 18.58 ± 0.4943 in wild-type and TREM2 deficient cells. N=50 MERCs. Data are represented as mean ± SEM and the statistical significance was $p < 0.001$.

Figure 5. The thickness of MERC in TREM2 deficient iMGL and the iMGL infected with TREM2 lentivirus.
(A) Transmission Electron microscopy (TEM) images of TREM2 deficient iMGL cells with control lentivirus (left), and TREM2 lentivirus (right). An increased number of LDs in TREM2-deficient iMGL was prominent, in contrast, LD was decreased in the cell infected with TREM2 lentivirus.
(B) Black squares are enlarged images from dotted rectangles showing MERC. Arrows showed MERC. (C) Increased thickness of MERC in TREM2 deficient iMGL was rescued by TREM2 encoding vector. Each averaged thickness (nm) of MERC was 19.52 ± 0.5512 and 14.1 ± 0.3741 in TREM2 deficient iMGL and the cell infected with TREM2 encoding vector. N=87 MERCs. Data are represented as mean ± SEM and the statistical significance was $p < 0.001$.

Figure 6. Increased thickness of MERC in TREM2 R47mutated iMGL.
(A) Transmission Electron microscopy (TEM) images of iMGL cells from wild type and patient with R47H mutation. Enlarged images from dotted boxes (Right) showed MERCs. (B) The thickness of MERCs was analyzed in isogenic wild type and TREM2 R47H mutated iMGL. Each averaged thickness (nm) of MERC was 14.36 ± 0.3996 and 17.96 ± 0.3982 in isogenic wild type and TREM2 R47H mutated iMGL. N=110. Data are represented as mean ± SEM and the statistical significance was $p < 0.001$.

REFERENCES

Abud EM, Ramirez RN, Martinez ES, Healy LM, Nguyen CHH, Newman SA, Yeromin AV, Scarfone VM, Marsh SE, Fimbres C, Caraway CA, Fote GM, Madany AM, Agrawal A, Kayed R, Gylys KH, Cahalan MD, Cummings BJ, Antel JP, Mortazavi A, Carson MJ, Poon WW, Blurton-Jones M. iPSC-Derived Human Microglia-like Cells to Study Neurological Diseases. Neuron. 2017 Apr 19;94(2):278-293. PMID: 28426964Area-Gomez E, de Groof A, Bonilla E, Montesinos J, Tanji K, Boldogh I, Pon L, Schon EA. A key role for MAM in mediating mitochondrial dysfunction in Alzheimer disease. Cell Death Dis. 2018 Feb 28;9(3):335. PMID: 29491396

Area-Gomez E, Del Carmen Lara Castillo M, Tambini MD, Guardia-Laguarta C, de Groof AJ, Madra M, Ikenouchi J, Umeda M, Bird TD, Sturley SL, Schon EA. Upregulated function of mitochondria-associated ER membranes in Alzheimer disease. EMBO J. 2012 Nov 5;31(21):4106-23. PMID: 22892566

Area-Gomez E, Schon EA. On the Pathogenesis of Alzheimer's Disease: The MAM Hypothesis. FASEB J. 2017 Mar;31(3):864-867. PMID: 28246299

Atagi Y, et al. Apolipoprotein E is a ligand for triggering receptor expressed on myeloid cells 2 (TREM2) J. Biol. Chem. 2015;290:26043–26050.

Bailey CC, DeVaux LB, Farzan M. The triggering receptor expressed on myeloid cells 2 binds apolipoprotein E. J. Biol. Chem. 2015;290:26033–26042.

Bartok, A., et al. IP3 receptor isoforms differently regulate ER-mitochondrial contacts and local calcium transfer. Nat Commun 10, 3726 (2019).

Batti L, Sundukova M, Murana E, Pimpinella S, De Castro Reis F, Pagani F, Wang H, Pellegrino E, Perlas E, Di Angelantonio S, Ragozzino D, Heppenstall PA. TMEM16F Regulates Spinal Microglial Function in Neuropathic Pain States. Cell Rep. 2016 Jun 21;15(12):2608-15. PMID: 27332874

Bludau I, Aebersold R. Proteomic and interactomic insights into the molecular basis of cell functional diversity. Nat Rev Mol Cell Biol. 2020 Jun;21(6):327-340. PMID: 32235894

Bose A, Beal MF. Mitochondrial dysfunction in Parkinson's disease. J Neurochem. 2016 Oct;139 Suppl 1:216-231. PMID: 27546335

Branon TC, Bosch JA, Sanchez AD, Udeshi ND, Svinkina T, Carr SA, Feldman JL, Perrimon N, Ting AY. Efficient proximity labeling in living cells and organisms with TurboID. Nat Biotechnol. 2018 Oct;36(9):880-887. PMID: 30125270

Chen F, Yan B, Ren J, Lyu R, Wu Y, Guo Y, Li D, Zhang H, Hu J. FIT2 organizes lipid droplet biogenesis with ER tubule-forming proteins and septins. J Cell Biol. 2021 May 3;220(5):e201907183. PMID: 33861319

Cheng-Hathaway PJ, Reed-Geaghan EG, Jay TR, Casali BT, Bemiller SM, Puntambekar SS, von Saucken VE, Williams RY, Karlo JC, Moutinho M, Xu G, Ransohoff RM, Lamb BT, Landreth GE. The Trem2 R47H variant confers loss-of-function-like phenotypes in Alzheimer's disease. Mol Neurodegener. 2018 Jun 1;13(1):29. PMID: 29859094

Choi CR, Rhee HW. Proximity labeling: an enzymatic tool for spatial biology. Trends Biotechnol. 2022 Feb;40(2):145-148. PMID: 34663510

Choudhary V, Schneiter R. A Unique Junctional Interface at Contact Sites Between the Endoplasmic Reticulum and Lipid Droplets. Front Cell Dev Biol. 2021 Apr 8;9:650186. PMID: 33898445

Colonna M. The biology of TREM receptors. Nat Rev Immunol. 2023 Feb 7:1-15. PMID: 36750615

492
493 Cosker K, Mallach A, Limaye J, Piers TM, Staddon J, Neame SJ, Hardy J, Pocock JM. Microglial
494 signalling pathway deficits associated with the patient derived R47H TREM2 variants linked to AD
495 indicate inability to activate inflammasome. Sci Rep. 2021 Jun 25;11(1):13316. PMID: 34172778
496
497 Csordás G., Renken C., Várnai P., Walter L., Weaver D., Buttle K. F., et al. (2006). Structural and
498 functional features and significance of the physical linkage between ER and mitochondria. J. Cell. Biol.
499 174, 915–921. PMID: 16982799
500
501 Cui ZQ, Hu XY, Yang T, Guan JW, Gu Y, Li HY, Zhang HY, Xiao QH, Sun XH. TMEM16F may be a new
502 therapeutic target for Alzheimer's disease. Neural Regen Res. 2023 Mar;18(3):643-651. PMID: 36018189
503
504 Doerr A. Proximity labeling with TurboID. Nat Methods. 2018 Oct;15(10):764. doi: 10.1038/s41592-018-
505 0158-0. PMID: 30275580
506
507 Freyre CAC, Rauher PC, Ejsing CS, Klemm RW. MIGA2 Links Mitochondria, the ER, and Lipid Droplets
508 and Promotes De Novo Lipogenesis in Adipocytes. Mol Cell. 2019 Dec 5;76(5):811-825.e14. PMID:
509 31628041
510
511 Fu WY, et al. Targeting Neuroinflammation as a Therapeutic Strategy for Alzheimer's Disease:
512 Mechanisms, Drug Candidates, and New Opportunities. ACS Chem Neurosci. 2019. PMID:30221933
513
514 Ghosh C, Das N, Saha S, Kundu T, Sircar D, Roy P. Involvement of Cdkal1 in the etiology of type 2
515 diabetes mellitus and microvascular diabetic complications: a review. J Diabetes Metab Disord. 2022 Jan
516 13;21(1):991-1001. PMID: 35673487
517
518 Giacomello M, Pellegrini L. The coming of age of the mitochondria-ER contact: a matter of thickness. Cell
519 Death Differ. 2016 Sep 1;23(9):1417-27. PMID: 27341186
520
521 Griciuc A, Tanzi RE. The role of innate immune genes in Alzheimer's disease. Curr Opin Neurol. 2021
522 Apr 1;34(2):228-236. PMID: 33560670
523
524 Guerreiro R, Wojtas A, Bras J, Carrasquillo M, Rogaeva E, Majounie E, Cruchaga C, Sassi C, Kauwe JS,
525 Younkin S, Hazrati L, Collinge J, Pocock J, Lashley T, Williams J, Lambert JC, Amouyel P, Goate A,
526 Rademakers R, Morgan K, Powell J, St George-Hyslop P, Singleton A, Hardy J; Alzheimer Genetic
527 Analysis Group. TREM2 variants in Alzheimer's disease. N Engl J Med. 2013 Jan 10;368(2):117-27.
528 PMID: 23150934
529
530 Guyard V, Monteiro-Cardoso VF, Omrane M, Sauvanet C, Houcine A, Boulogne C, Ben Mbarek K, Vitale
531 N, Faklaris O, El Khallouki N, Thiam AR, Giordano F. ORP5 and ORP8 orchestrate lipid droplet
532 biogenesis and maintenance at ER-mitochondria contact sites. J Cell Biol. 2022 Sep
533 5;221(9):e202112107. PMID: 35969857
534
535 Han S, Li J, Ting AY. Proximity labeling: spatially resolved proteomic mapping for neurobiology. Curr
536 Opin Neurobiol. 2018 Jun;50:17-23. PMID: 29125959
537
538 Hansen DV, Hanson JE, Sheng M. Microglia in Alzheimer's disease. J Cell Biol. 2018 Feb 5;217(2):459-
539 472. PMID: 29196460
540
541 Herold C, Hooli BV, Mullin K, Liu T, Roehr JT, Mattheisen M, Parrado AR, Bertram L, Lange C, Tanzi RE.
542 Family-based association analyses of imputed genotypes reveal genome-wide significant association of
543 Alzheimer's disease with OSBPL6, PTPRG, and PDCL3. Mol Psychiatry. 2016 Nov;21(11):1608-1612.
544 PMID: 26830138
545
546 Horng T. Calcium signaling and mitochondrial destabilization in the triggering of the nlrp3 inflammasome.
547 Trends Immunol. 2014;35:253–261.PMID: 24646829

548
549 Jay TR, von Saucken VE, Landreth GE. TREM2 in Neurodegenerative Diseases. Mol Neurodegener.
550 2017 Aug 2;12(1):56. PMID: 28768545
551
552 Jiang W, Liu F, Li H, Wang K, Cao X, Xu X, Zhou Y, Zou J, Zhang X, Cui X. TREM2 ameliorates
553 anesthesia and surgery-induced cognitive impairment by regulating mitophagy and NLRP3
554 inflammasome in aged C57/BL6 mice. Neurotoxicology. 2022 May;90:216-227. PMID:35447280
555
556 Johri A, Chandra A. Connection Lost, MAM: Errors in ER-Mitochondria Connections in
557 Neurodegenerative Diseases. Brain Sci. 2021 Oct 28;11(11):1437. PMID: 34827436
558
559 Jonsson T, Stefansson H, Steinberg S, Jonsdottir I, Jonsson PV, Snaedal J, Bjornsson S, Huttenlocher J,
560 Levey AI, Lah JJ, Rujescu D, Hampel H, Giegling I, Andreassen OA, Engedal K, Ulstein I, Djurovic S,
561 Ibrahim-Verbaas C, Hofman A, Ikram MA, van Duijn CM, Thorsteinsdottir U, Kong A, Stefansson K.
562 Variant of TREM2 associated with the risk of Alzheimer's disease. N Engl J Med. 2013 Jan
563 10;368(2):107-16. PMID: 23150908
564
565 Jorfi M, Maaser-Hecker A, Tanzi RE. The neuroimmune axis of Alzheimer's disease. Genome Med. 2023
566 Jan 26;15(1):6. PMID: 36703235
567
568 Keren-Shaul H, et al. A unique microglia type associated with restricting development of Alzheimer's
569 disease. Cell. 2017;169:1276–1290.e17. PMID: 28602351
570
571 Kleinberger G, Yamanishi Y, Suarez-Calvet M, Czirr E, Lohmann E, Cuyvers E et al. TREM2 mutations
572 implicated in neurodegeneration impair cell surface transport and phagocytosis. Sci Transl Med 2014; 6:
573 243ra86. [PubMed] [Google Scholar] PMID: 24990881
574
575 Klunemann, H. H. et al. The genetic causes of basal ganglia calcification, dementia, and bone cysts:
576 DAP12 and TREM2. Neurology 64, 1502–1507 (2005).
577
578 Kober DL, Brett TJ. TREM2-Ligand Interactions in Health and Disease. J Mol Biol. 2017 Jun
579 2;429(11):1607-1629. PMID: 28432014
580
581 Krasemann S, et al. The TREM2–APOE pathway drives the transcriptional phenotype of dysfunctional
582 microglia in neurodegenerative diseases. Immunity. 2017;47:566–581. PMID: 28930663
583
584 Kunzelmann K, Nilius B, Owsianik G, Schreiber R, Ousingsawat J, Sirianant L, Wanitchakool P, Bevers
585 EM, Heemskerk JW. Molecular functions of anoctamin 6 (TMEM16F): a chloride channel, cation channel,
586 or phospholipid scramblase? Pflugers Arch. 2014 Mar;466(3):407-14. doi: 10.1007/s00424-013-1305-1.
587 PMID: 23748496
588
589 Kwak C, Shin S, Park JS, Jung M, Nhung TTM, Kang MG, Lee C, Kwon TH, Park SK, Mun JY, Kim JS,
590 Rhee HW. Contact-ID, a tool for profiling organelle contact sites, reveals regulatory proteins of
591 mitochondrial-associated membrane formation. Proc Natl Acad Sci U S A. 2020 Jun 2;117(22):12109-
592 12120. PMID: 32414919
593
594 Lam SS, Martell JD, Kamer KJ, Deerinck TJ, Ellisman MH, Mootha VK, Ting AY. Directed evolution of
595 APEX2 for electron microscopy and proximity labeling. Nat Methods. 2015 Jan;12(1):51-4. PMID:
596 25419960
597
598 Lanier LL. DAP10- and DAP12-associated receptors in innate immunity. Immunol Rev. 2009
599 Jan;227(1):150-60. PMID: 19120482
600
601 Lee S, Min KT. The Interface Between ER and Mitochondria: Molecular Compositions and Functions. Mol
602 Cells. 2018 Dec 31;41(12):1000-1007. PMID: 30590907
603

Lee SY, Seo JK, Rhee HW. Direct Identification of Biotinylated Proteins from Proximity Labeling (Spot-BioID). Methods Mol Biol. 2019;2008:97-105. PMID: 31124091

Lemke G. How macrophages deal with death. Nat Rev Immunol. 2019 Sep;19(9):539-549. PMID: 31019284

Leng F, Edison P.Neuroinflammation and microglial activation in Alzheimer disease: where do we go from here? Nat Rev Neurol. 2021 Mar;17(3):157-172. PMID: 33318676

Lessard CB, et al. High-affinity interactions and signal transduction between Aβ oligomers and TREM2. EMBO Mol. Med. 2018;10:e9027. PMID: 30341064

Li Y, Long W, Gao M, Jiao F, Chen Z, Liu M, Yu L. TREM2 Regulates High Glucose-Induced Microglial Inflammation via the NLRP3 Signaling Pathway. Brain Sci. 2021 Jul 7;11(7):896. PMID: 34356130

Liu L, Zhang K, Sandoval H, Yamamoto S, Jaiswal M, Sanz E, Li Z, Hui J, Graham BH, Quintana A, Bellen HJ. Glial lipid droplets and ROS induced by mitochondrial defects promote neurodegeneration. Cell. 2015 Jan 15;160(1-2):177-90. PMID: 25594180

Matarin M, Salih DA, Yasvoina M, Cummings DM, Guelfi S, Liu W, Nahaboo Solim MA, Moens TG, Paublete RM, Ali SS, Perona M, Desai R, Smith KJ, Latcham J, Fulleylove M, Richardson JC, Hardy J, Edwards FA. A genome-wide gene-expression analysis and database in transgenic mice during development of amyloid or tau pathology. Cell Rep. 2015 Feb 3;10(4):633-44.

Mazzeo A, Porta M, Beltramo E. Characterization of an Immortalized Human Microglial Cell Line as a Tool for the Study of Diabetic Retinopathy. Int J Mol Sci. 2022 May 20;23(10):5745. PMID: 35628555

McQuade A, Blurton-Jones M. Microglia in Alzheimer's Disease: Exploring How Genetics and Phenotype Influence Risk. J Mol Biol. 2019 Apr 19;431(9):1805-1817. PMID: 30738892

McQuade A, Coburn M, Tu CH, Hasselmann J, Davtyan H, Blurton-Jones M. Development and validation of a simplified method to generate human microglia from pluripotent stem cells. Mol Neurodegener. 2018 Dec 22;13(1):67. PMID: 30577865

Nugent AA, Lin K, van Lengerich B, Lianoglou S, Przybyla L, Davis SS, Llapashtica C, Wang J, Kim DJ, Xia D, Lucas A, Baskaran S, Haddick PCG, Lenser M, Earr TK, Shi J, Dugas JC, Andreone BJ, Logan T, Solanoy HO, Chen H, Srivastava A, Poda SB, Sanchez PE, Watts RJ, Sandmann T, Astarita G, Lewcock JW, Monroe KM, Di Paolo G. TREM2 Regulates Microglial Cholesterol Metabolism upon Chronic Phagocytic Challenge. Neuron. 2020 Mar 4;105(5):837-854.e9. PMID: 31902528

Olzmann, J.A.; Carvalho, P. Dynamics and functions of lipid droplets. Nat. Rev. Mol. Cell Biol. 2019, 20, 137–155

Paillusson S, Stoica R, Gomez-Suaga P, Lau DHW, Mueller S, Miller T, Miller CCJ. There's Something Wrong with my MAM; the ER-Mitochondria Axis and Neurodegenerative Diseases. Trends Neurosci. 2016 Mar;39(3):146-157. PMID: 26899735

Paloneva, J. et al. Mutations in two genes encoding different subunits of a receptor signaling complex result in an identical disease phenotype. Am. J. Hum. Genet. 71, 656–662 (2002).
Park JS, Ji IJ, An HJ, Kang MJ, Kang SW, Kim DH et al. Disease-associated mutations of TREM2 alter the processing of N-linked oligosaccharides in the Golgi apparatus. Traffic 2015; 16: 510–518. PMID: 25615530

Qin W, Cho KF, Cavanagh PE, Ting AY. Deciphering molecular interactions by proximity labeling. Nat Methods. 2021 Feb;18(2):133-143. PMID: 33432242

660 Raturi A., et al. TMX1 determines cancer cell metabolism as a thiol-based modulator of ER-mitochondria
661 Ca2+ flux. J Cell Biol. 2016 Aug 15;214(4):433-44.
662
663 Rees JS, Li XW, Perrett S, Lilley KS, Jackson AP. Protein neighbors and proximity proteomics. MCP.
664 2015;14(11):2848–56. PMID: 26355100
665
666 Rieusset J. Mitochondria-associated membranes (MAMs): An emerging platform connecting energy and
667 immune sensing to metabolic flexibility. Biochem Biophys Res Commun. 2018 May 27;500(1):35-44.
668 PMID: 28647358
669
670 Robichaud S, Fairman G, Vijithakumar V, Mak E, Cook DP, Pelletier AR, Huard S, Vanderhyden BC,
671 Figeys D, Lavallée-Adam M, Baetz K, Ouimet M. Identification of novel lipid droplet factors that regulate
672 lipophagy and cholesterol efflux in macrophage foam cells. Autophagy. 2021 Nov;17(11):3671-3689.
673 PMID: 33590792
674
675 Sarlus H, Heneka MT. Microglia in Alzheimer's disease. J Clin Invest. 2017 Sep 1;127(9):3240-3249.
676 PMID: 28862638
677
678 Scott-Hewitt N, Perrucci F, Morini R, Erreni M, Mahoney M, Witkowska A, Carey A, Faggiani E, Schuetz
679 LT, Mason S, Tamborini M, Bizzotto M, Passoni L, Filipello F, Jahn R, Stevens B, Matteoli M. Local
680 externalization of phosphatidylserine mediates developmental synaptic pruning by microglia. EMBO J.
681 2020 Aug 17;39(16):e105380. PMID: 32657463
682
683 Simino J, Wang Z, Bressler J, Chouraki V, Yang Q, Younkin SG, Seshadri S, Fornage M, Boerwinkle E,
684 Mosley TH Jr. Whole exome sequence-based association analyses of plasma amyloid-β in African and
685 European Americans; the Atherosclerosis Risk in Communities-Neurocognitive Study. PLoS One. 2017
686 Jul 13;12(7):e0180046. PMID: 28704393
687
688 Song W, et al. Alzheimer's disease-associated TREM2 variants exhibit either decreased or increased
689 ligand-dependent activation. Alzheimers Dement. 2017;13:381–387. PMID: 27520774
690
691 Sudom A, Talreja S, Danao J, Bragg E, Kegel R, Min X, Richardson J, Zhang Z, Sharkov N, Marcora E,
692 Thibault S, Bradley J, Wood S, Lim AC, Chen H, Wang S, Foltz IN, Sambashivan S, Wang Z. Molecular
693 basis for the loss-of-function effects of the Alzheimer's disease-associated R47H variant of the immune
694 receptor TREM2. J Biol Chem. 2018 Aug 10;293(32):12634-12646. PMID: 29794134
695
696 Takahashi K, Rochford CD, Neumann H. Clearance of apoptotic neurons without inflammation by
697 microglial triggering receptor expressed on myeloid cells-2. J. Exp. Med. 2005;201:647–657. PMID:
698 15728241
699
700 Tubbs E, Rieusset J. (2017) Metabolic signaling functions of ER-mitochondria contact sites: role in
701 metabolic diseases. J Mol Endocrinol 58, R87-R106. PMID: 27965371
702
703 Vance JE. MAM (mitochondria-associated membranes) in mammalian cells: lipids and beyond. Biochim
704 Biophys Acta. 2014 Apr 4;1841(4):595-609. PMID: 24316057
705
706 Vance JE. Phospholipid synthesis in a membrane fraction associated with mitochondria. J Biol Chem
707 1990 May 5;265(13):7248-56. PMID: 2332429
708
709 Villegas-Llerena C, Phillips A, Garcia-Reitboeck P, Hardy J, Pocock JM. Microglial genes regulating
710 neuroinflammation in the progression of Alzheimer's disease. Curr Opin Neurobiol. 2016 Feb;36:74-81.
711 PMID: 26517285
712
713 Wang Y, Cao C, Zhu Y, Fan H, Liu Q, Liu Y, Chen K, Wu Y, Liang S, Li M, Li L, Liu X, Zhang Y, Wu C, Lu
714 G, Wu M. TREM2/β-catenin attenuates NLRP3 inflammasome-mediated macrophage pyroptosis to

715 promote bacterial clearance of pyogenic bacteria. Cell Death Dis. 2022 Sep 6;13(9):771. PMID:
716 36068223
717
718 Wyss-Coray T, Mucke L. Inflammation in neurodegenerative disease--a double-edged sword. Neuron.
719 2002;35:419–432. doi: 10.1016/S0896-6273(02)00794-8.
720
721 Yang H, Kim A, David T, Palmer D, Jin T, Tien J, Huang F, Cheng T, Coughlin SR, Jan YN, Jan LY.
722 TMEM16F forms a Ca2+-activated cation channel required for lipid scrambling in platelets during blood
723 coagulation. Cell. 2012 Sep 28;151(1):111-22. PMID: 23021219
724
725 Yin J, Liu X, He Q, Zhou L, Yuan Z, Zhao S. Vps35-dependent recycling of Trem2 regulates microglial
726 function. Traffic. 2016 Dec;17(12):1286-1296. PMID: 27717139
727
728 Zampese E, Fasolato C, Kipanyula MJ, Bortolozzi M, Pozzan T, Pizzo P. Presenilin 2 modulates
729 endoplasmic reticulum (ER)-mitochondria interactions and Ca2+ cross-talk. Proc Natl Acad Sci U S A.
730 2011 Feb 15;108(7):2777-82. PMID: 21285369
731
732 Zhang B, Gaiteri C, Bodea LG, Wang Z, McElwee J, Podtelezhnikov AA, Zhang C, Xie T, Tran L, Dobrin
733 R, Fluder E, Clurman B, Melquist S, Narayanan M, Suver C, Shah H, Mahajan M, Gillis T, Mysore J,
734 MacDonald ME, Lamb JR, Bennett DA, Molony C, Stone DJ, Gudnason V, Myers AJ, Schadt EE,
735 Neumann H, Zhu J, Emilsson V. Integrated systems approach identifies genetic nodes and networks in
736 late-onset Alzheimer's disease. Cell. 2013 Apr 25;153(3):707-20. PMID: 23622250
737
738 Zhang L, Feng XK, Ng YK, Li SC. Reconstructing directed gene regulatory network by only gene
739 expression data. BMC Genomics. 2016 Aug 18;17 Suppl 4:430. PMID: 27556418
740
741 Zhang Y, Li H, Li X, Wu J, Xue T, Wu J, Shen H, Li X, Shen M, Chen G. TMEM16F Aggravates Neuronal
742 Loss by Mediating Microglial Phagocytosis of Neurons in a Rat Experimental Cerebral Ischemia and
743 Reperfusion Model. Front Immunol. 2020 Jul 7;11:1144. PMID: 32733436
744
745 Zhao Y, et al. TREM2 is a receptor for beta-amyloid that mediates microglial function. Neuron.
746 2018;97:1023–1031. PMID: 29518356
747
748 Zhao Y, Li X, Huang T, Jiang LL, Tan Z, Zhang M, Cheng IH, Wang X, Bu G, Zhang YW, Wang Q, Xu H.
749 Intracellular trafficking of TREM2 is regulated by presenilin 1. Exp Mol Med. 2017 Dec 1;49(12):e405.
750 PMID: 29611543
751
752 Zhong L, et al. Amyloid-beta modulates microglial responses by binding to the triggering receptor
753 expressed on myeloid cells 2 (TREM2) Mol. Neurodegener. 2018;13:15. PMID: 29587871
754
755 Zhou Y, Tada M, Cai Z, Andhey PS, Swain A, Miller KR, Gilfillan S, Artyomov MN, Takao M, Kakita A,
756 Colonna M. Human early-onset dementia caused by DAP12 deficiency reveals a unique signature of
757 dysregulated microglia. Nat Immunol. 2023 Mar;24(3):545-557. PMID: 36658241
758
759 Zhou Y, Tong Z, Jiang S, Zheng W, Zhao J, Zhou X. The Roles of Endoplasmic Reticulum in NLRP3
760 Inflammasome Activation. Cells. 2020 May 14;9(5):1219. PMID: 32423023

Figure 1

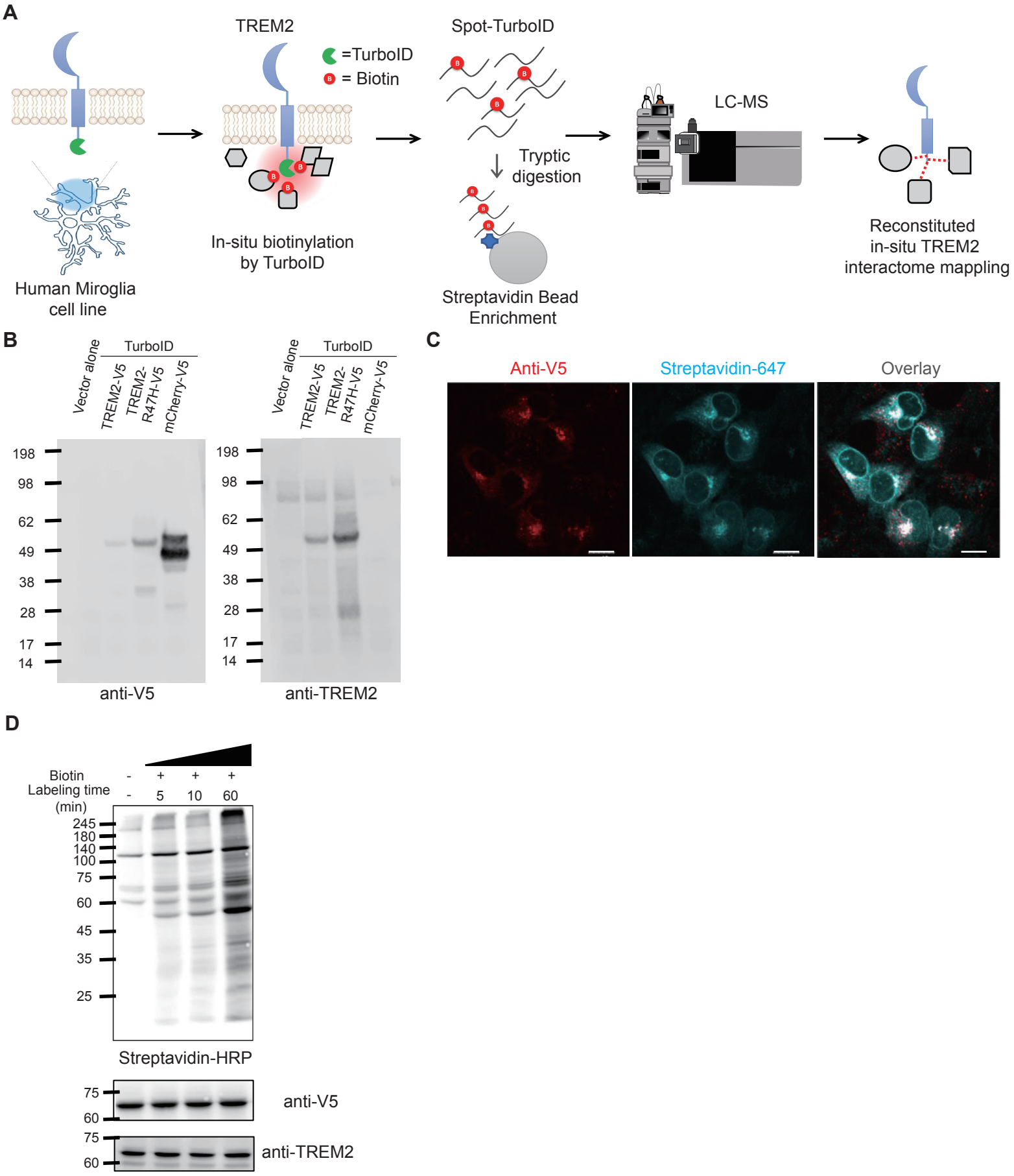
A
TREM2
=TurboID
= Biotin
Spot-TurboID
LC-MS
Tryptic digestion
Human Miroglia cell line
In-situ biotinylation by TurboID
Streptavidin Bead Enrichment
Reconstituted in-situ TREM2 interactome mappling
B
TurboID
Vector alone
TREM2-V5
TREM2-R47H-V5
mCherry-V5
198
98
62
49
38
28
17
14
anti-V5
anti-TREM2
C
Anti-V5
Streptavidin-647
Overlay
D
Biotin
Labeling time (min)
- + + +
- 5 10 60
245
180
140
100
75
60
45
35
25
Streptavidin-HRP
anti-V5
anti-TREM2

Figure 2

A

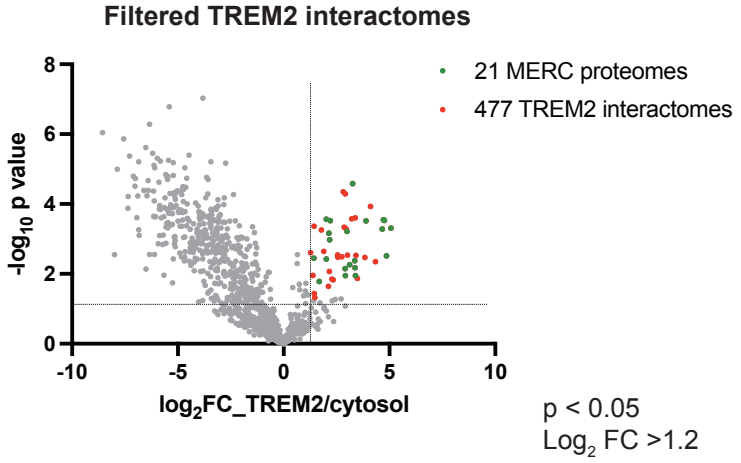
Filtered TREM2 interactomes
21 MERC proteomes
477 TREM2 interactomes
-log10 p value
log2FC_TREM2/cytosol
8
6
4
2
0
-10
-5
0
5
10
p < 0.05
Log2 FC >1.2

B

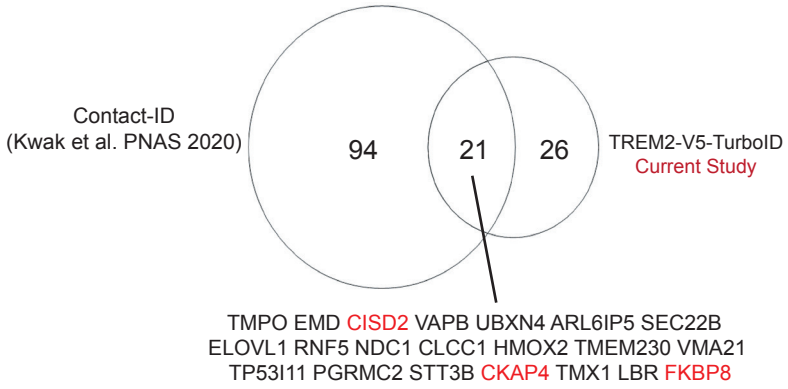
Contact-ID
(Kwak et al. PNAS 2020)
94
21
26
TREM2-V5-TurboID
Current Study
TMPO EMD CISD2 VAPB UBXN4 ARL6IP5 SEC22B
ELOVL1 RNF5 NDC1 CLCC1 HMOX2 TMEM230 VMA21
TP53I11 PGRMC2 STT3B CKAP4 TMX1 LBR FKBP8

C

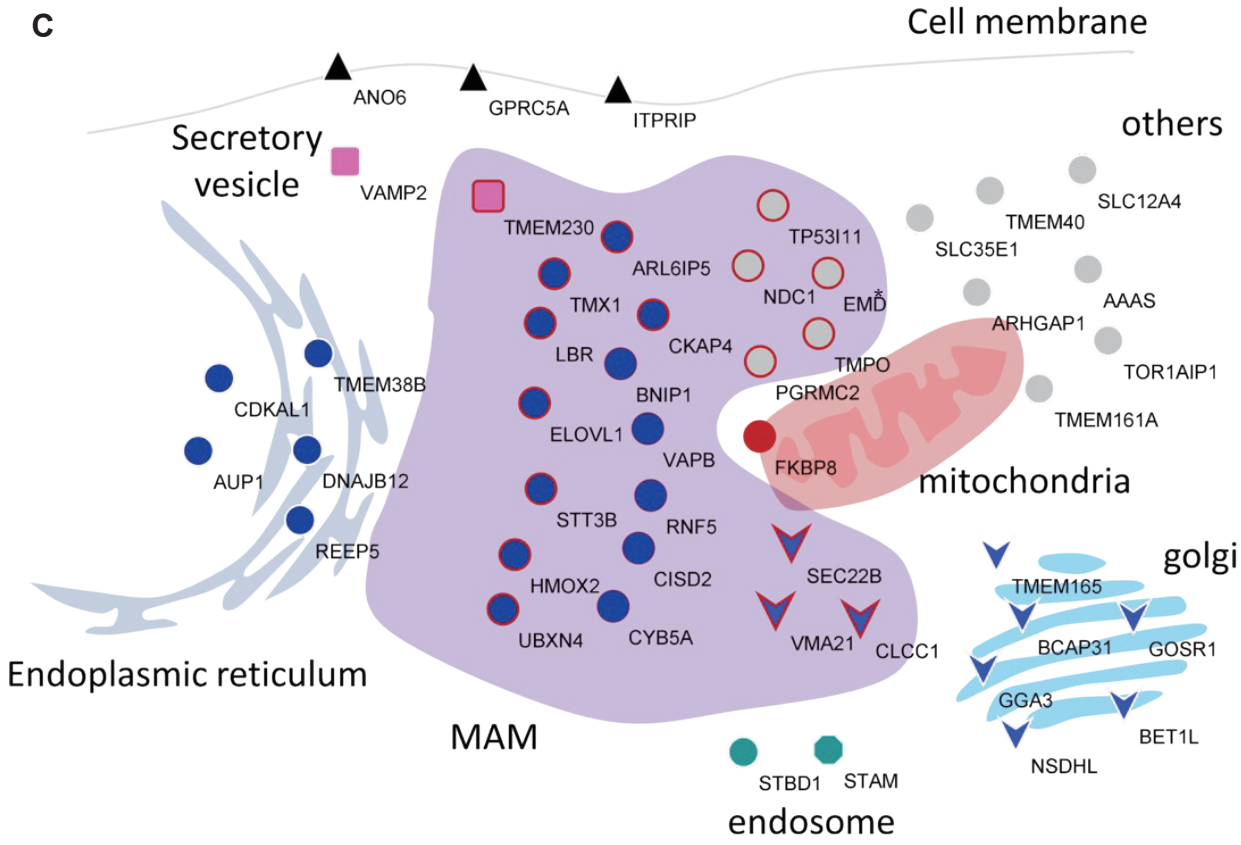
Cell membrane
ANO6
GPRC5A
ITPRIP
Secretory vesicle
VAMP2
others
SLC12A4
TMEM40
SLC35E1
AAAS
ARHGAP1
TOR1AIP1
TMEM161A
TMEM230
ARL6IP5
TP53I11
NDC1
EMD
TMX1
CKAP4
LBR
TMPO
PGRMC2
BNIP1
ELOVL1
VAPB
FKBP8
TMEM38B
CDKAL1
AUP1
DNAJB12
REEP5
STT3B
RNF5
HMOX2
CISD2
UBXN4
CYB5A
SEC22B
VMA21
CLCC1
mitochondria
golgi
TMEM165
BCAP31
GOSR1
GGA3
BET1L
NSDHL
Endoplasmic reticulum
MAM
STBD1
STAM
endosome

Figure 3

A

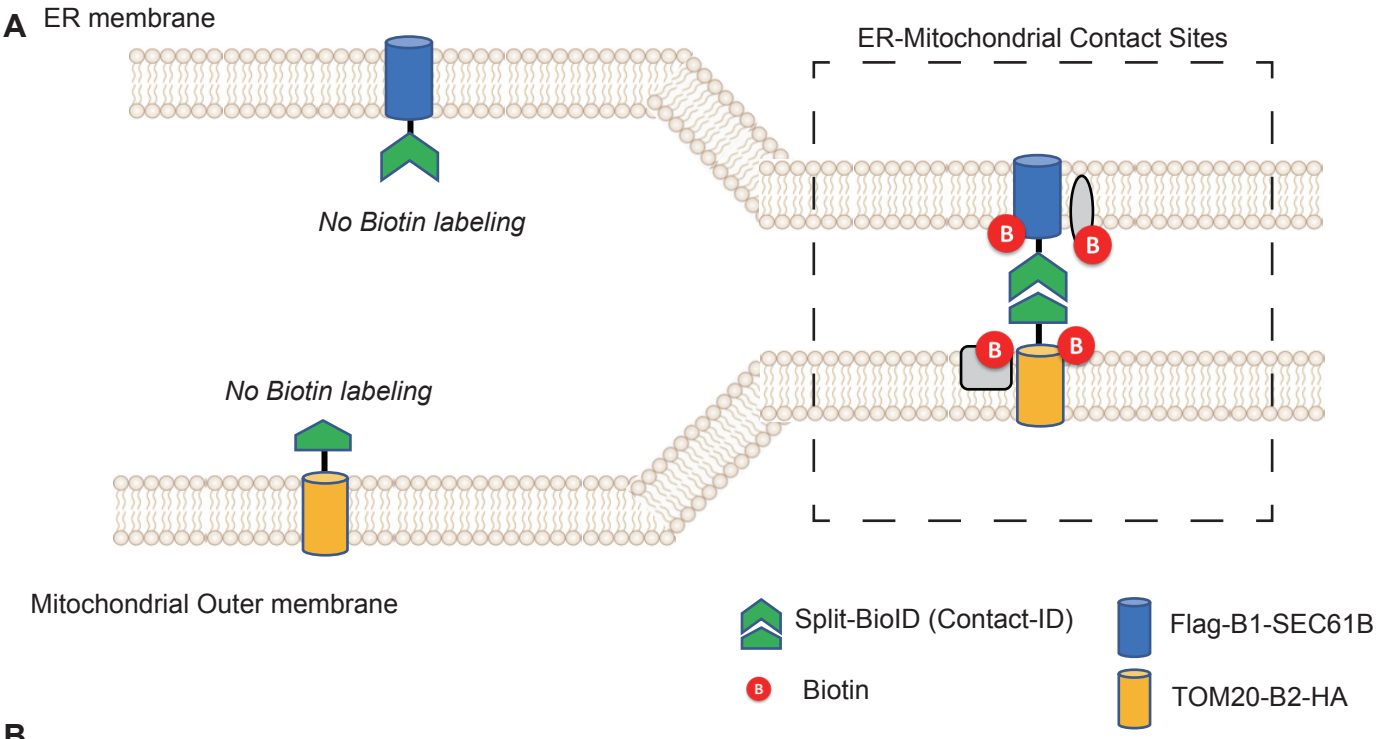
ER membrane
ER-Mitochondrial Contact Sites
No Biotin labeling
No Biotin labeling
Mitochondrial Outer membrane
Split-BioID (Contact-ID)
Flag-B1-SEC61B
Biotin
TOM20-B2-HA

B

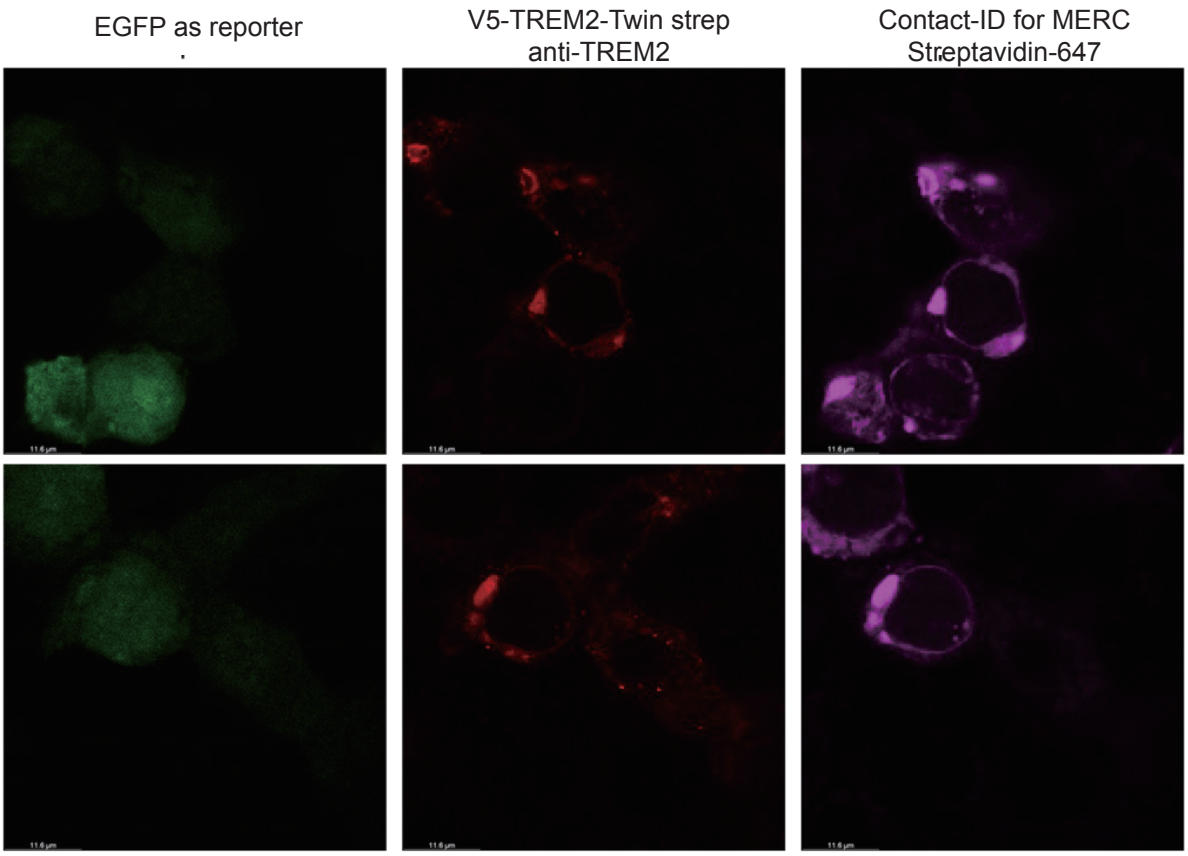
EGFP as reporter
V5-TREM2-Twin strep
anti-TREM2
Contact-ID for MERC
Streptavidin-647

C

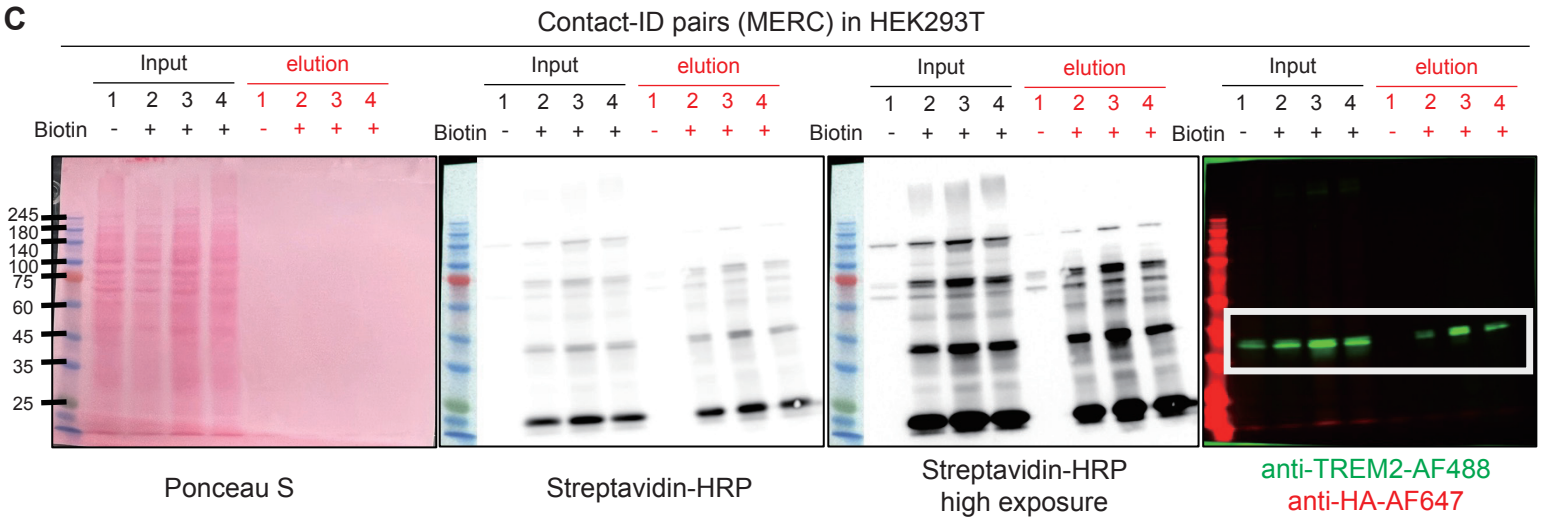
Contact-ID pairs (MERC) in HEK293T
Input
elution
1 2 3 4 1 2 3 4
Biotin - + + + - + + +
245
180
140
100
75
60
45
35
25
Ponceau S
Streptavidin-HRP
Streptavidin-HRP
high exposure
anti-TREM2-AF488
anti-HA-AF647

Figure 4

A

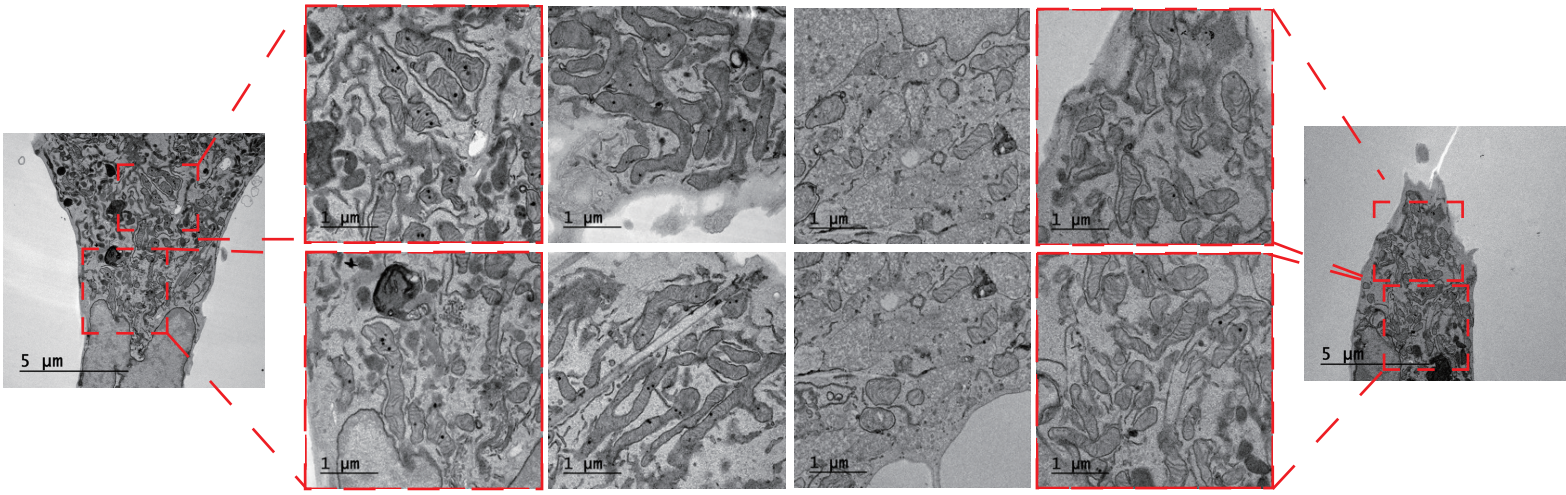

B

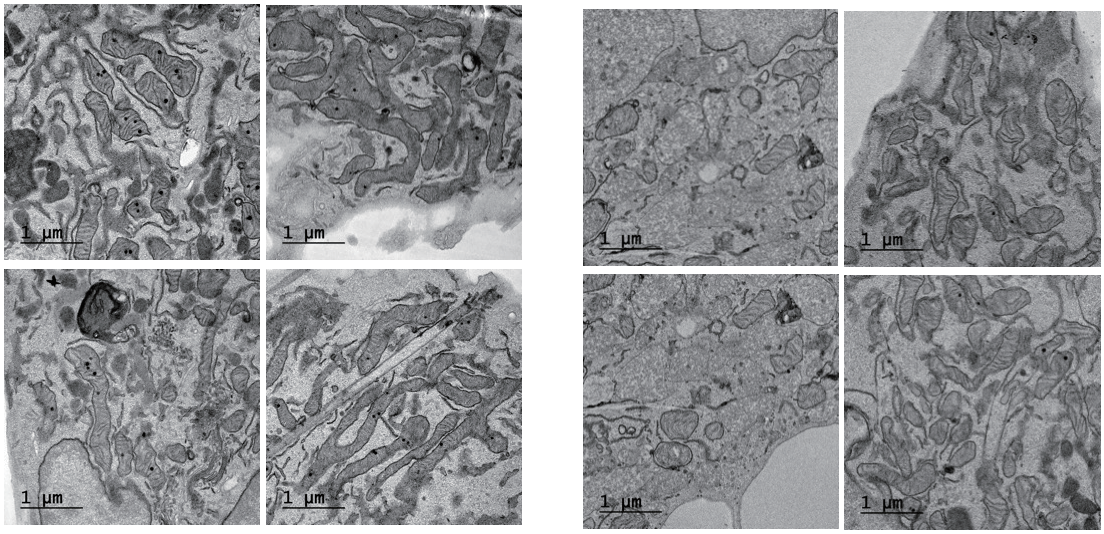

C

MERCs analysis

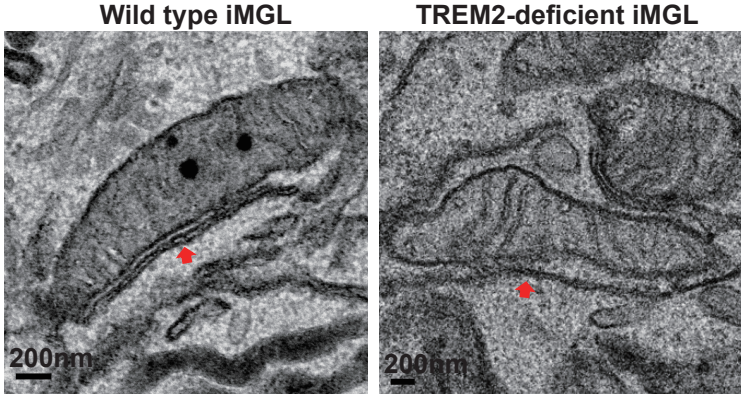

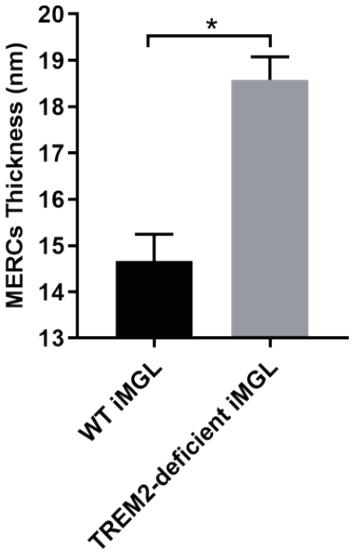

Tickness (nm)	WT iMGL	TREM2-deficient iMGL
AVE	14.66 ± 0.5874	18.58 ± 0.4943

Figure 5

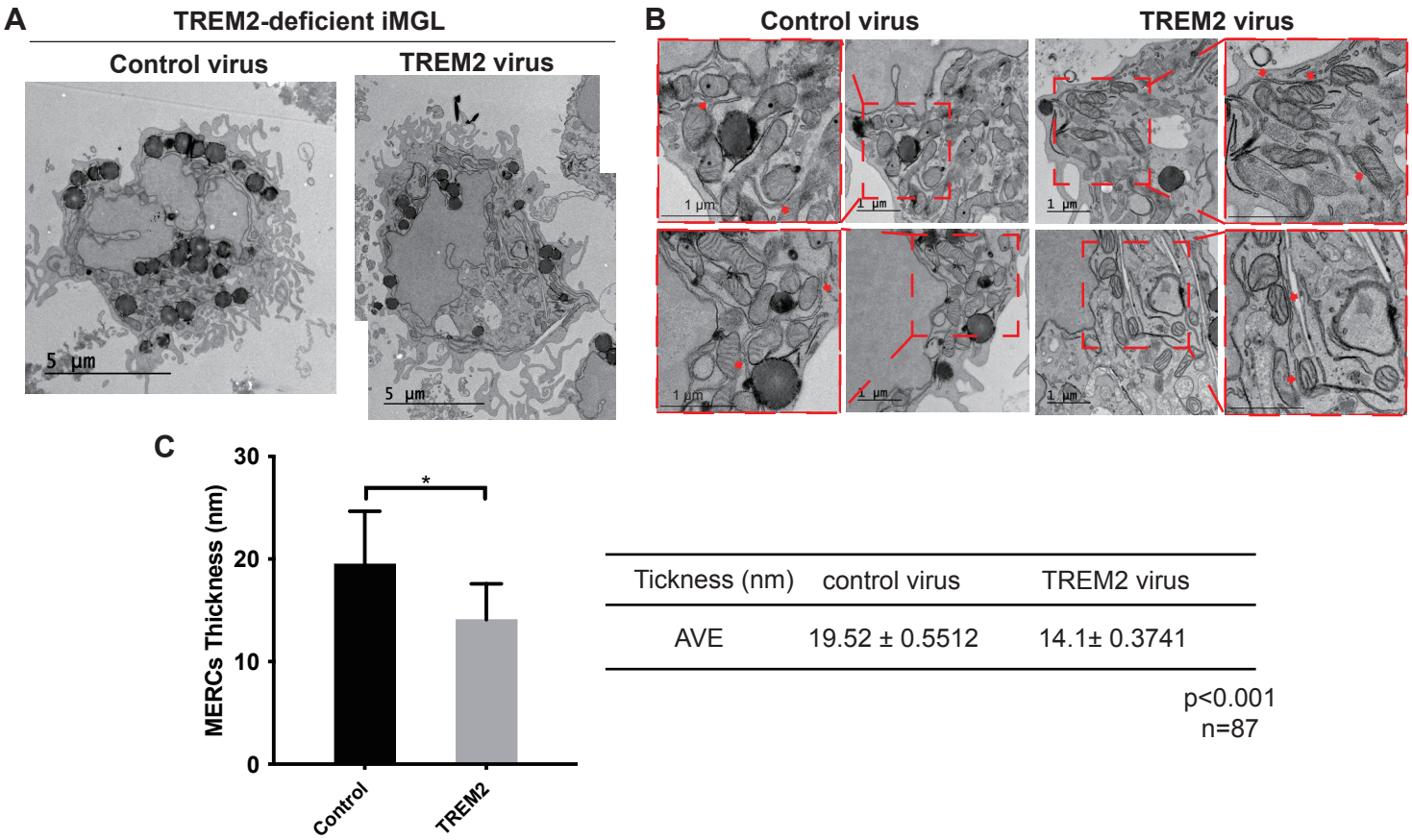

Tickness (nm)	control virus	TREM2 virus
AVE	19.52 ± 0.5512	14.1± 0.3741

$p<0.001$
n=87

Figure 6

A

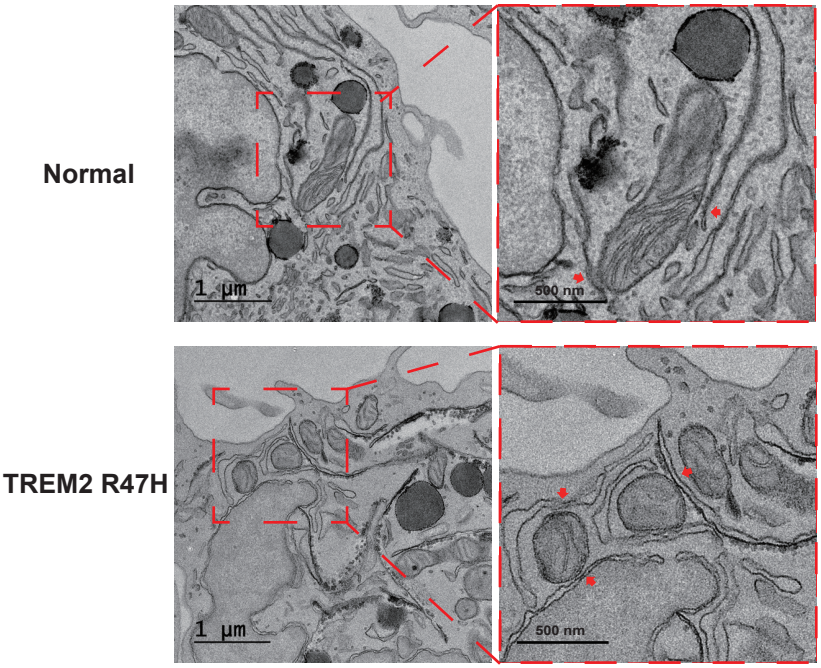

B

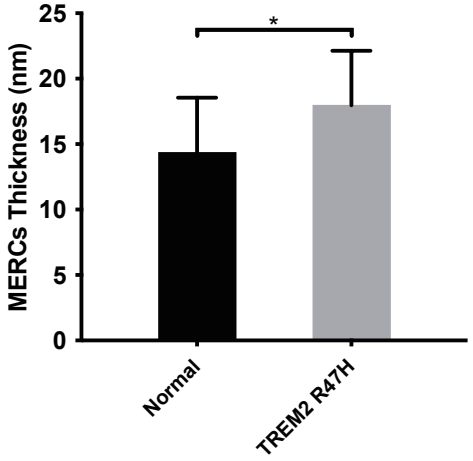

Tickness (nm)	Normal	TREM2 R47H
AVE	14.36± 0.3996	17.96± 0.3982

$p<0.001$
n=110

Figure S1

A

Expression constructs encoding:

TREM2-V5-TurboID Candidate #1, #2, ...

Co-transfection

HEK293T

In-situ biotinylation assay for validastion

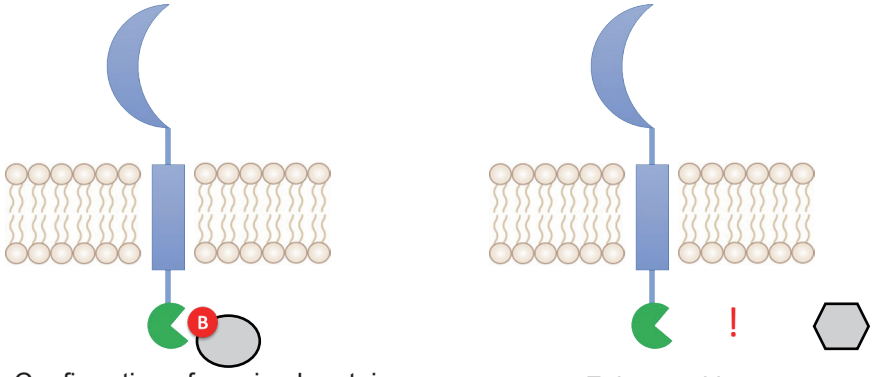

Confirmation of proximal protein (biotin-labeling)

False-positive (no biotin-labeling)

B

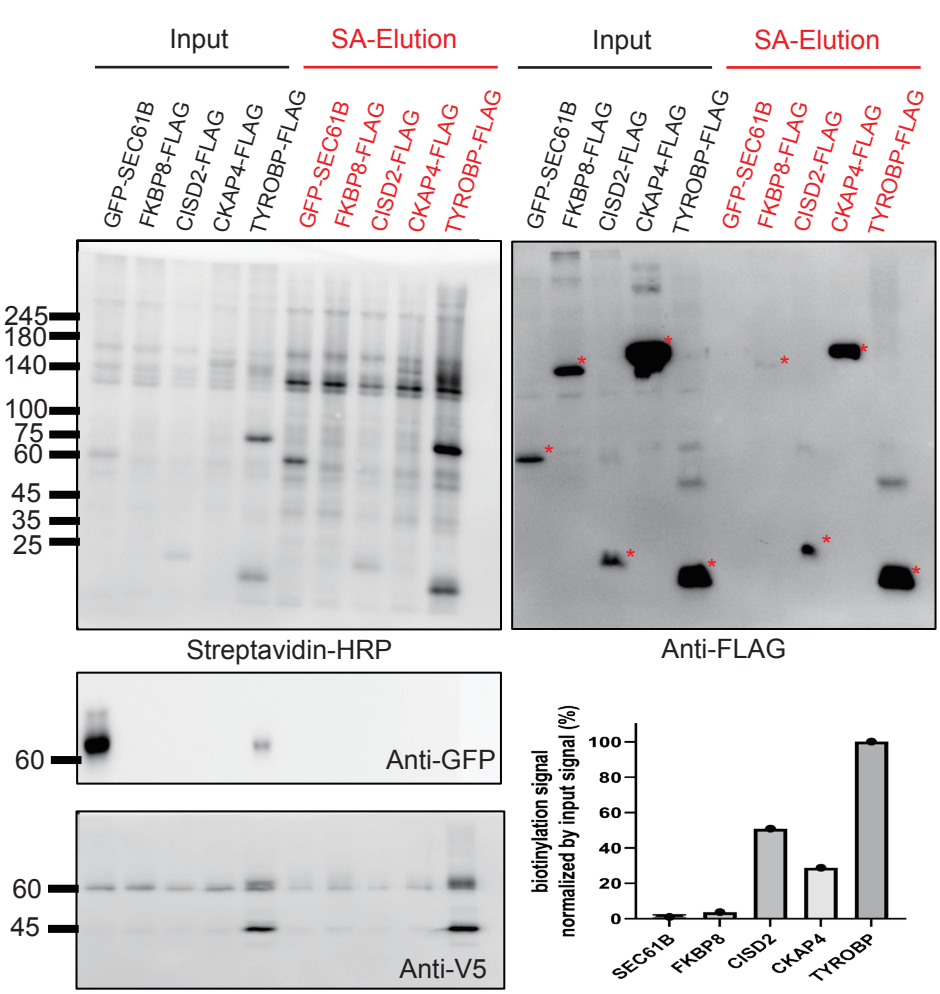

Figure S2

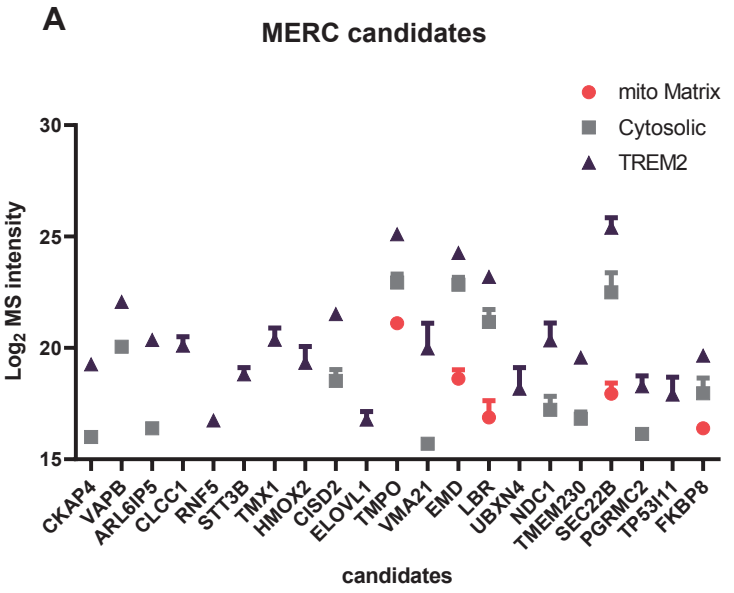
A
MERC candidates
mito Matrix
Cytosolic
TREM2
Log2 MS intensity
30
25
20
15
CKAP4
VAPB
ARL6IP5
CLCC1
RNF5
STT3B
TMX1
HMOX2
CISD2
ELOVL1
TMPO
VMA21
EMD
LBR
UBXN4
NDC1
TMEM230
SEC22B
PGRMC2
TP53I11
FKBP8
candidates

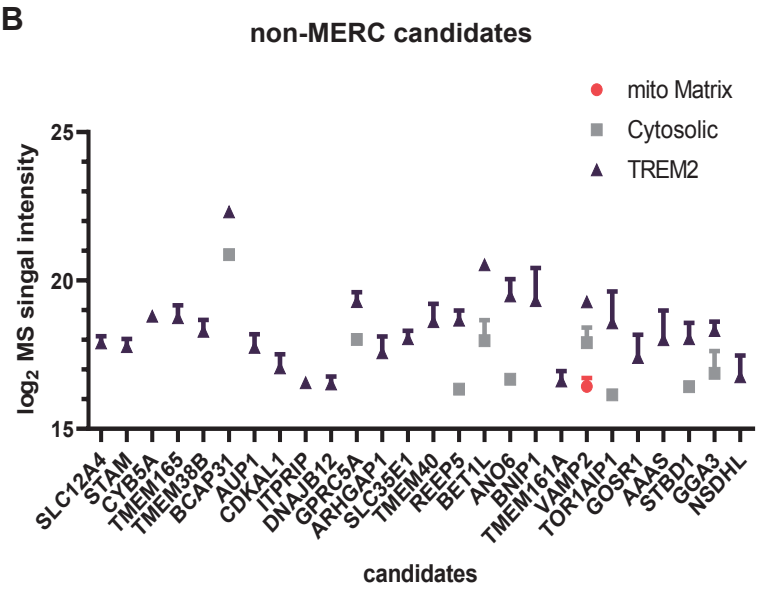
B
non-MERC candidates
mito Matrix
Cytosolic
TREM2
log2 MS singal intensity
25
20
15
SLC12A4
STAM
CYB5A
TMEM165
TMEM38B
BCAP31
AUP1
CDKAL1
ITPRIP
DNAJB12
GPRC5A
ARHGAP1
SLC35E1
TMEM40
REEP5
BET1L
ANO6
BNIP1
TMEM161A
VAMP2
TOR1AIP1
GOSR1
AAAS
STBD1
GGA3
NSDHL
candidates

Figure S3

A

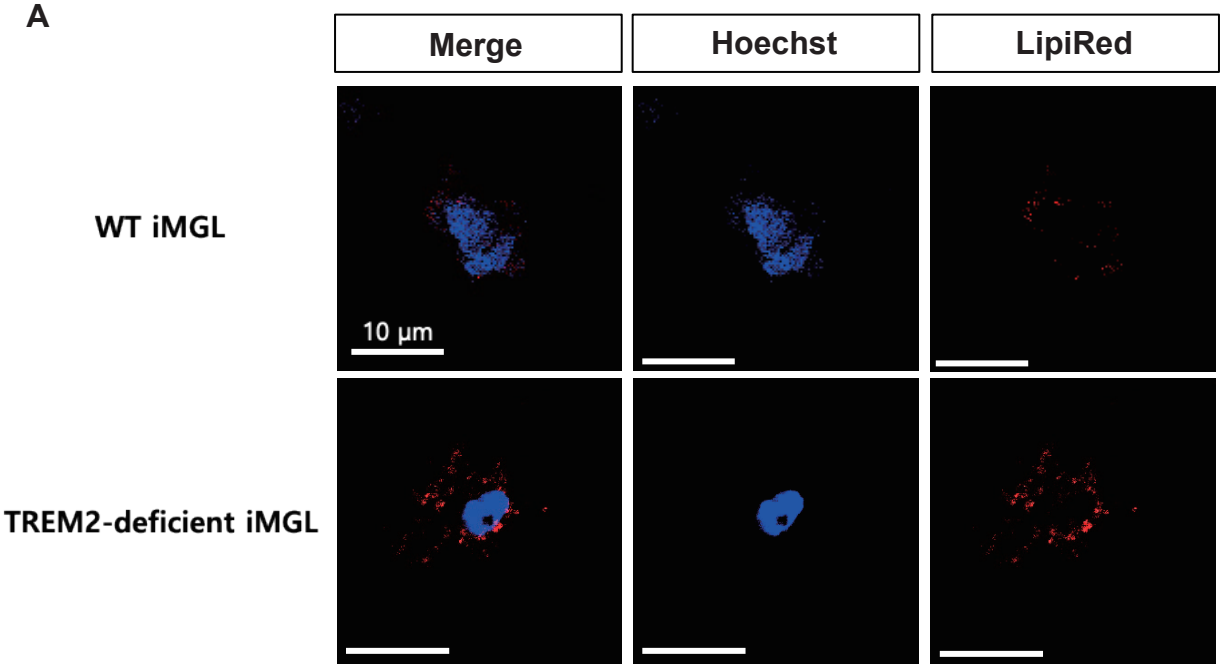

B

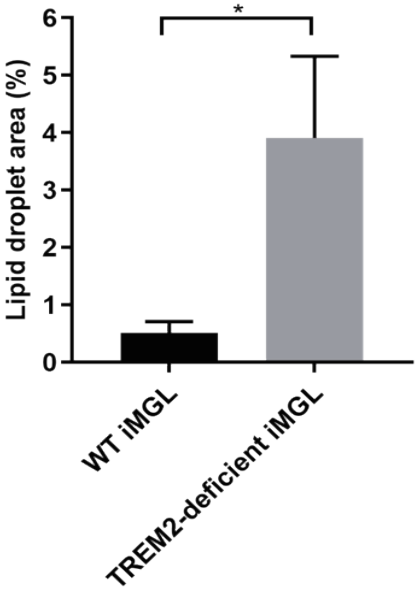

Tickness (nm)	WT iMGL	TREM2-deficient iMGL
AVE	0.513 ± 0.195	3.906± .427

$p<0.05$
n=9

Figure S4

A

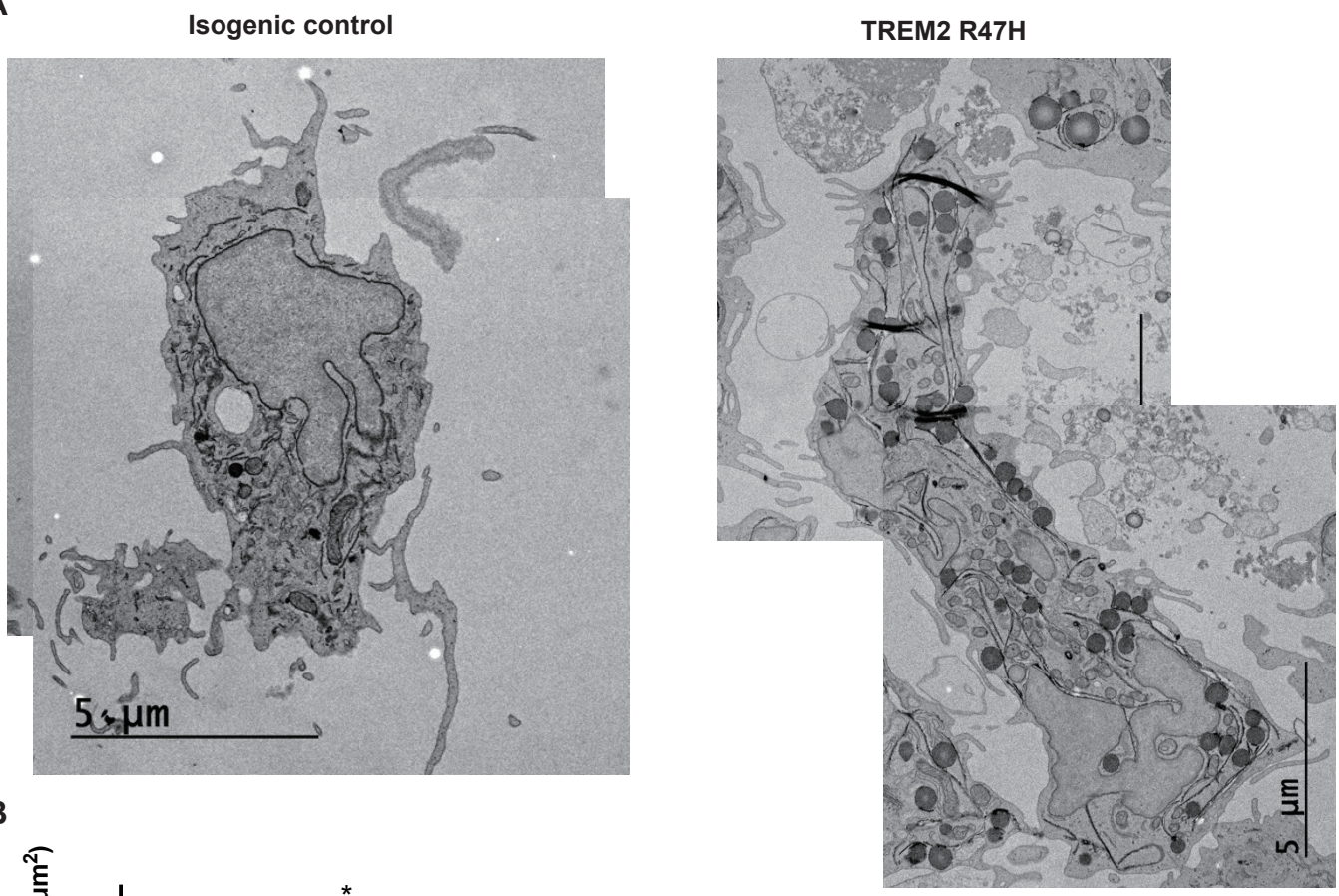

B

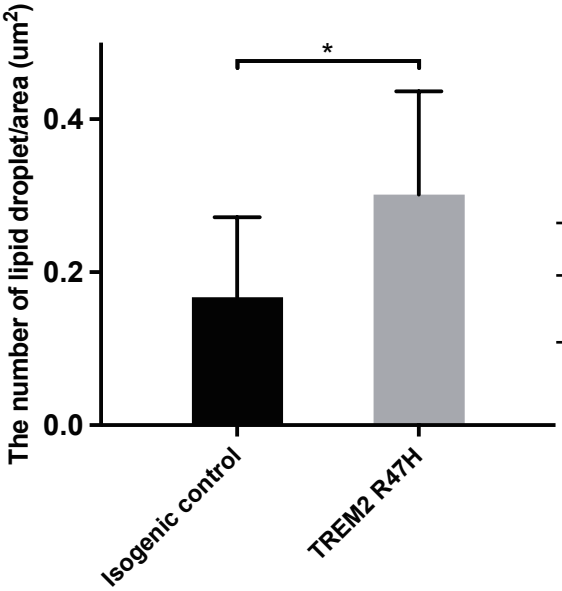

Tickness (nm)	Isogenic control	TREM2 R47H
AVE	0.1672± 0.370	0.3015±0.477

$p<0.05$
n=8